# Supplementary Information File

# Characterizing and controlling the inflammatory network during influenza A virus infection

Suoqin Jin[1], Yuanyuan Li[1], Ruangang Pan[2], Xiufen Zou[1]

[1]School of Mathematics and Statistics, Wuhan University, Wuhan 430072, China. [2]State Key Laboratory of Virology, College of Life Sciences, Wuhan University, Wuhan 430072, China.

## Table of Contents

**Supplementary Figures:**

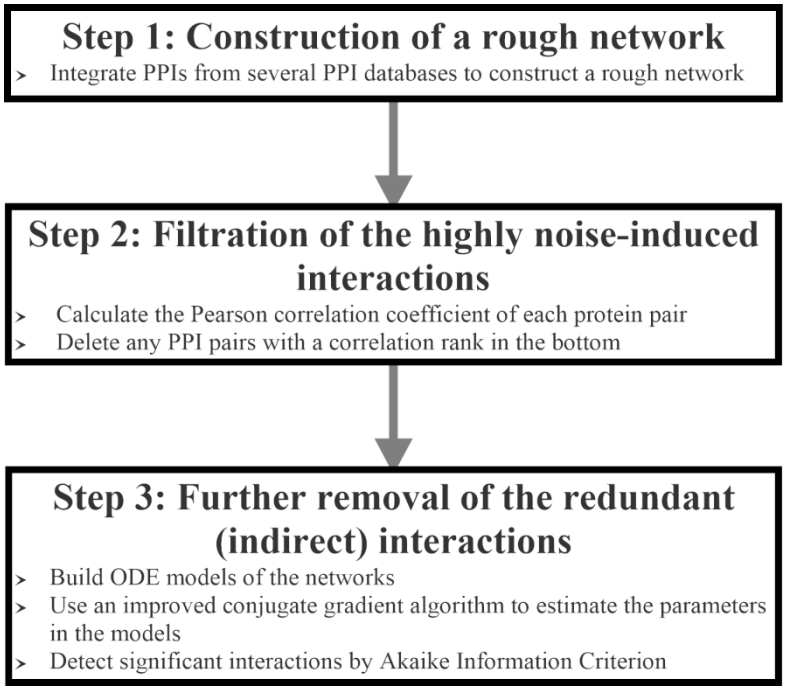


**Figure S1 | The framework of the network construction.**

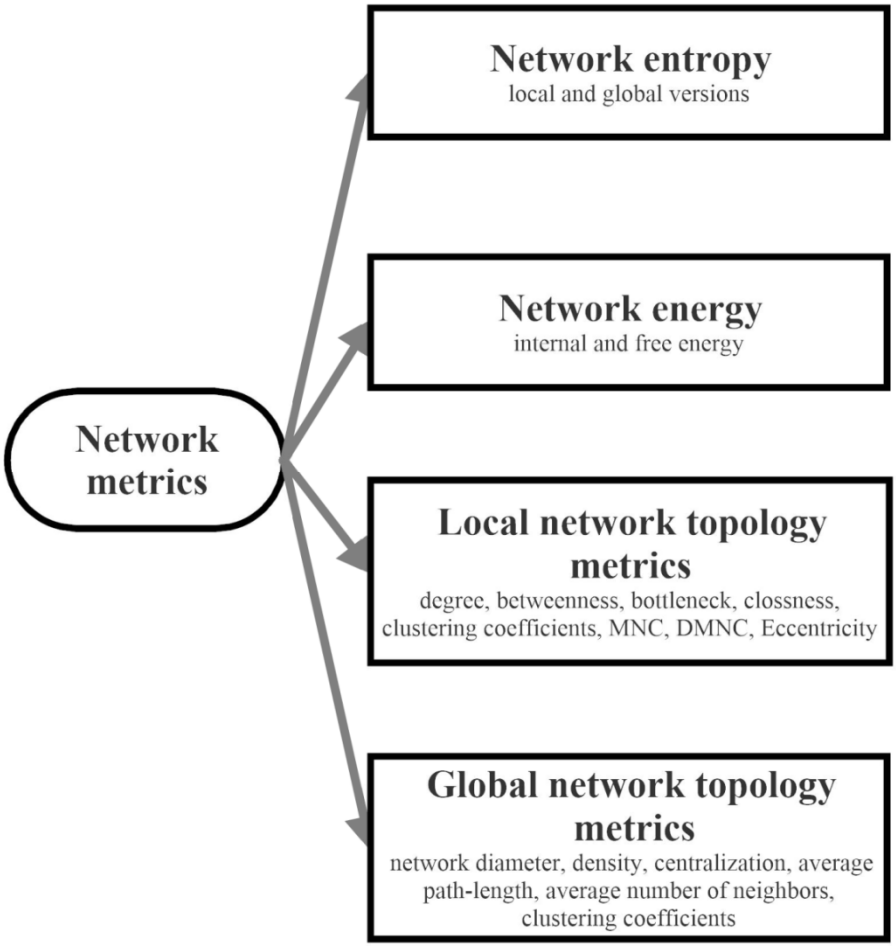


**Figure S2 | Network metrics explored in this study.** These network metrics were used to compare the network features of the inflammatory network with those of the normal network and then to characterize the inflammatory network.

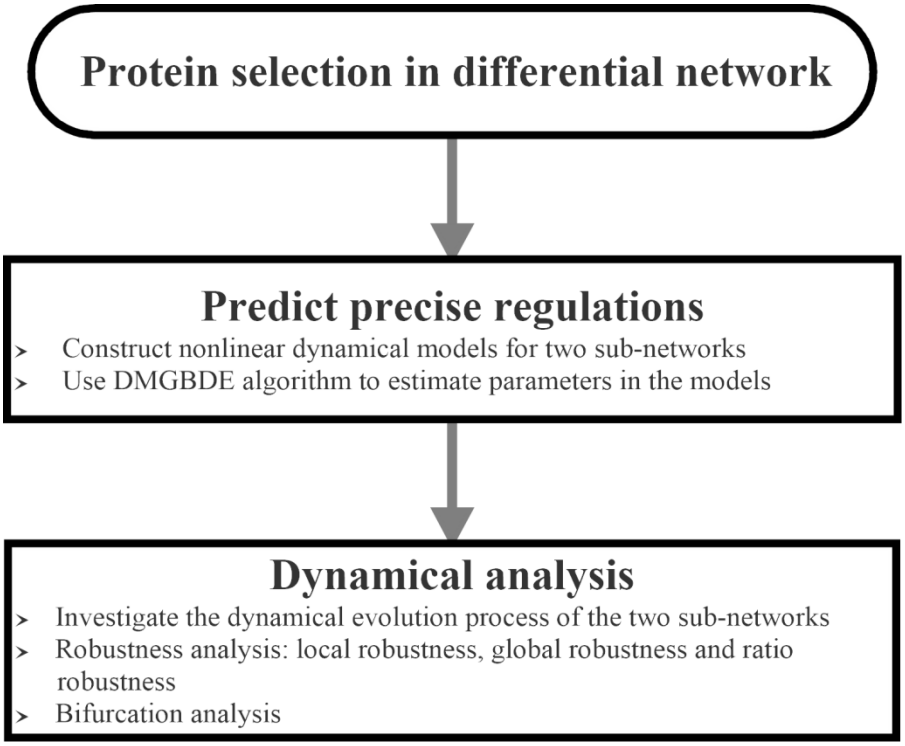


**Figure S3 | The procedure for dynamical analysis of the networks.**

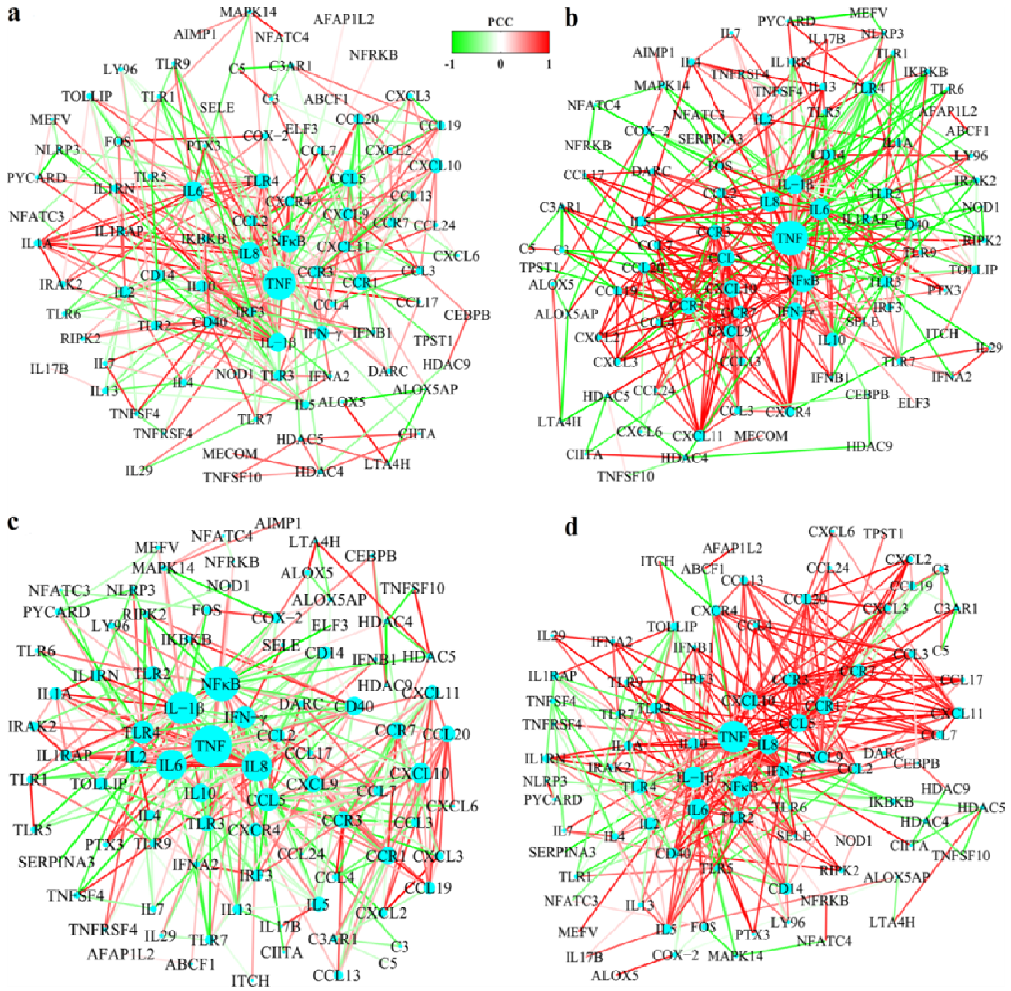


**Figure S4 | The constructed PPI networks during the H5N1 and H1N1 infections.** The node sizes are proportional to the degree of the nodes. The edge colors represent the Pearson correlation coefficient (PCC) of paired proteins (dark green and red indicate strong negative and positive correlations, respectively). (a) and (b) are the normal and inflammatory networks during the H5N1 infection, respectively. (c) and (d) are the normal and inflammatory networks during the H1N1 infection, respectively.

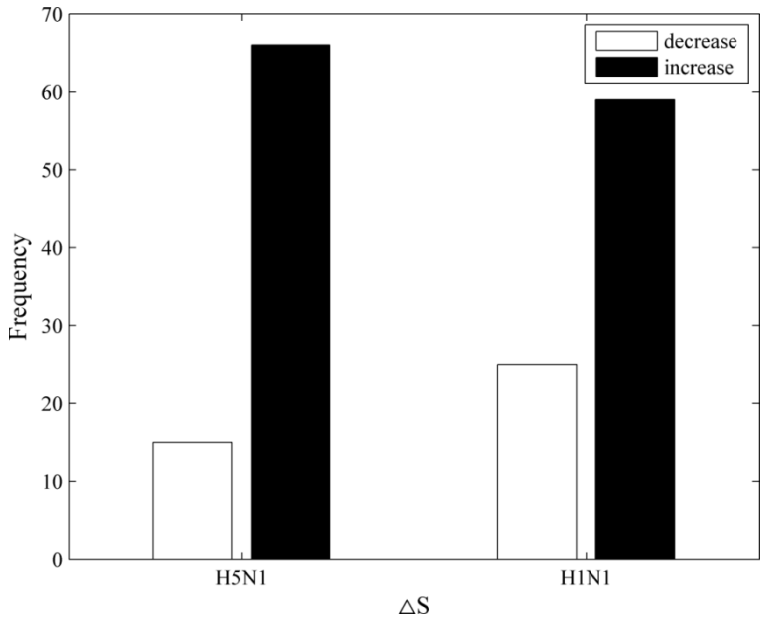


**Figure S5 | Comparison of the number of decreased and increased differential entropy values.** The number of increased differential entropies (66 for the H5N1 infection and 59 for the H1N1 infection) is significantly greater than the number of decreased differential entropies (15 for H5N1 infection and 25 for H1N1 infection).

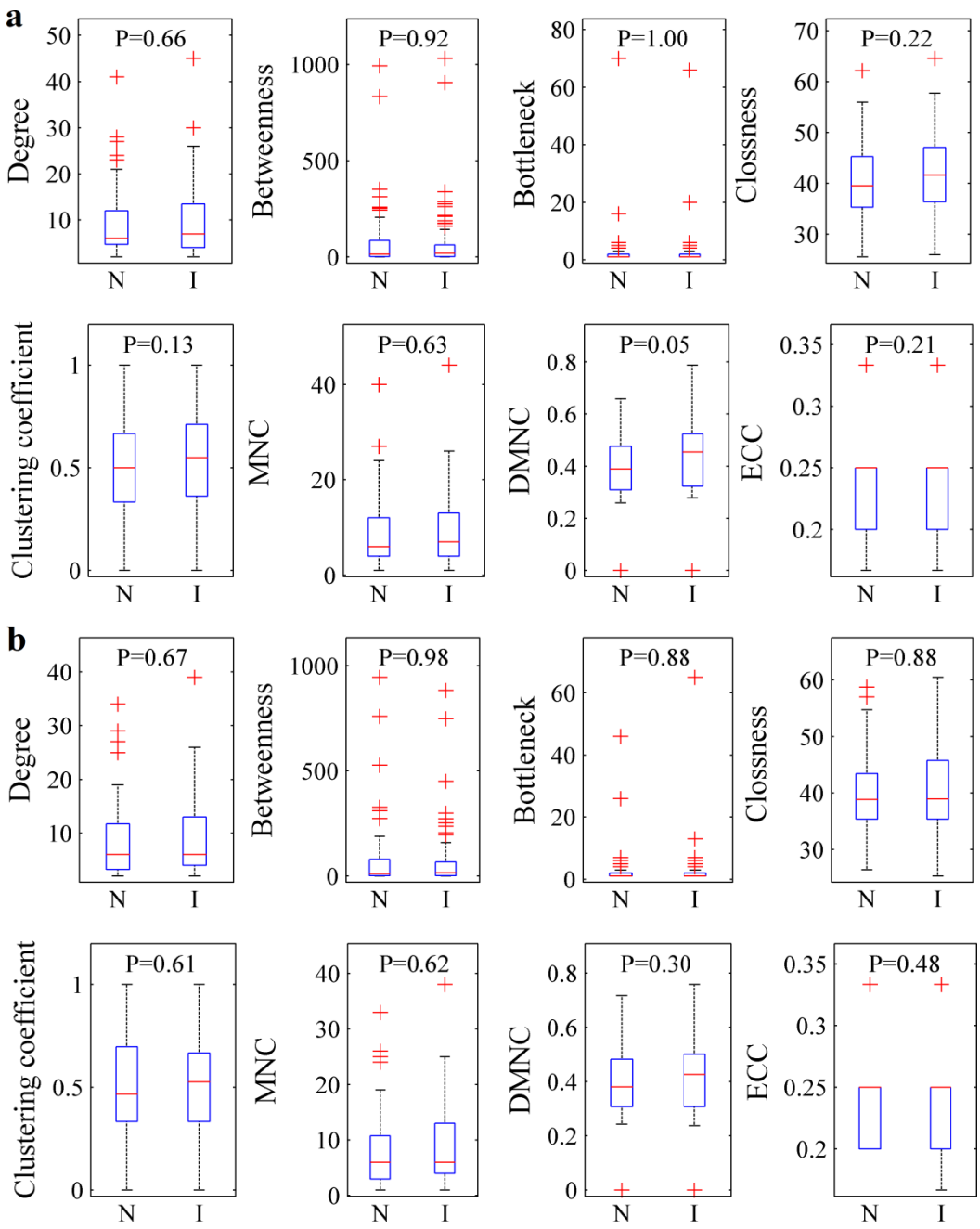


**Figure S6 | Comparison between the inflammatory (I) and normal (N) networks of eight local network metrics for all nodes with degree ≥2.** (a) H5N1 infection. (b) H1N1 infection. P-values are from a two-tailed Wilcoxon rank sum test.

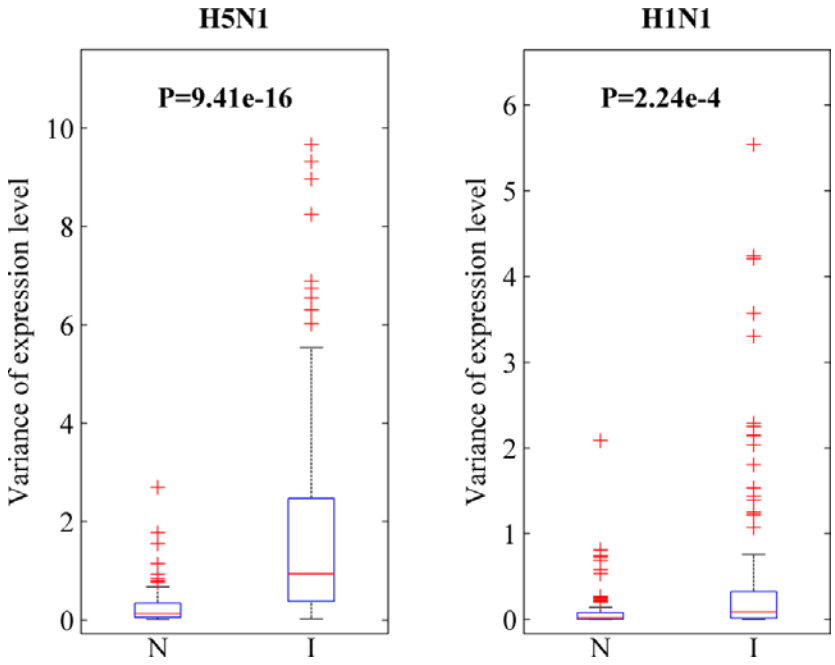


**Figure S7 | Comparison of the variance of protein expression levels between the inflammatory (I) and normal (N) networks.** The inflammatory networks exhibits significantly higher variability in the protein expression levels than that in the normal networks for the H5N1 and H1N1 infections. P-values are from an one-tailed Wilcoxon rank sum test.

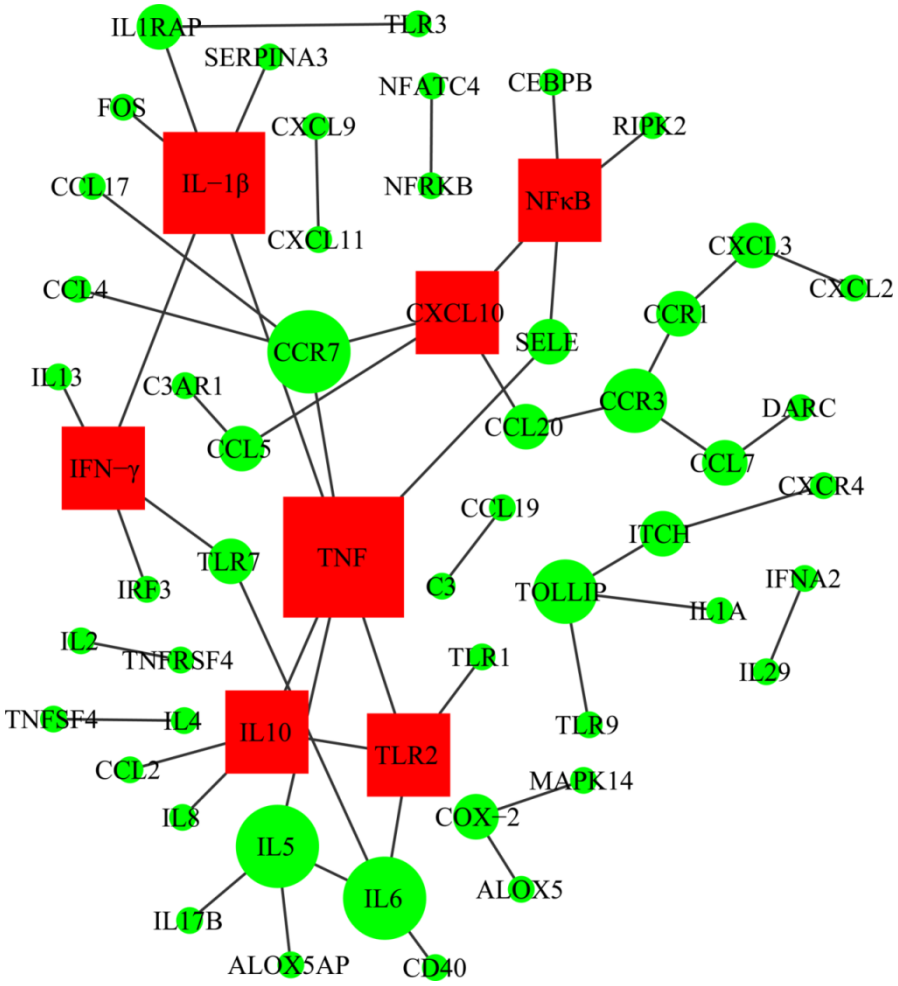


**Figure S8 | The differential network (edges are only in the inflammatory network and not in the normal network).** The node sizes are proportional to the degree of the nodes. The red square nodes represent the potential target proteins, which were selected for further dynamical analysis

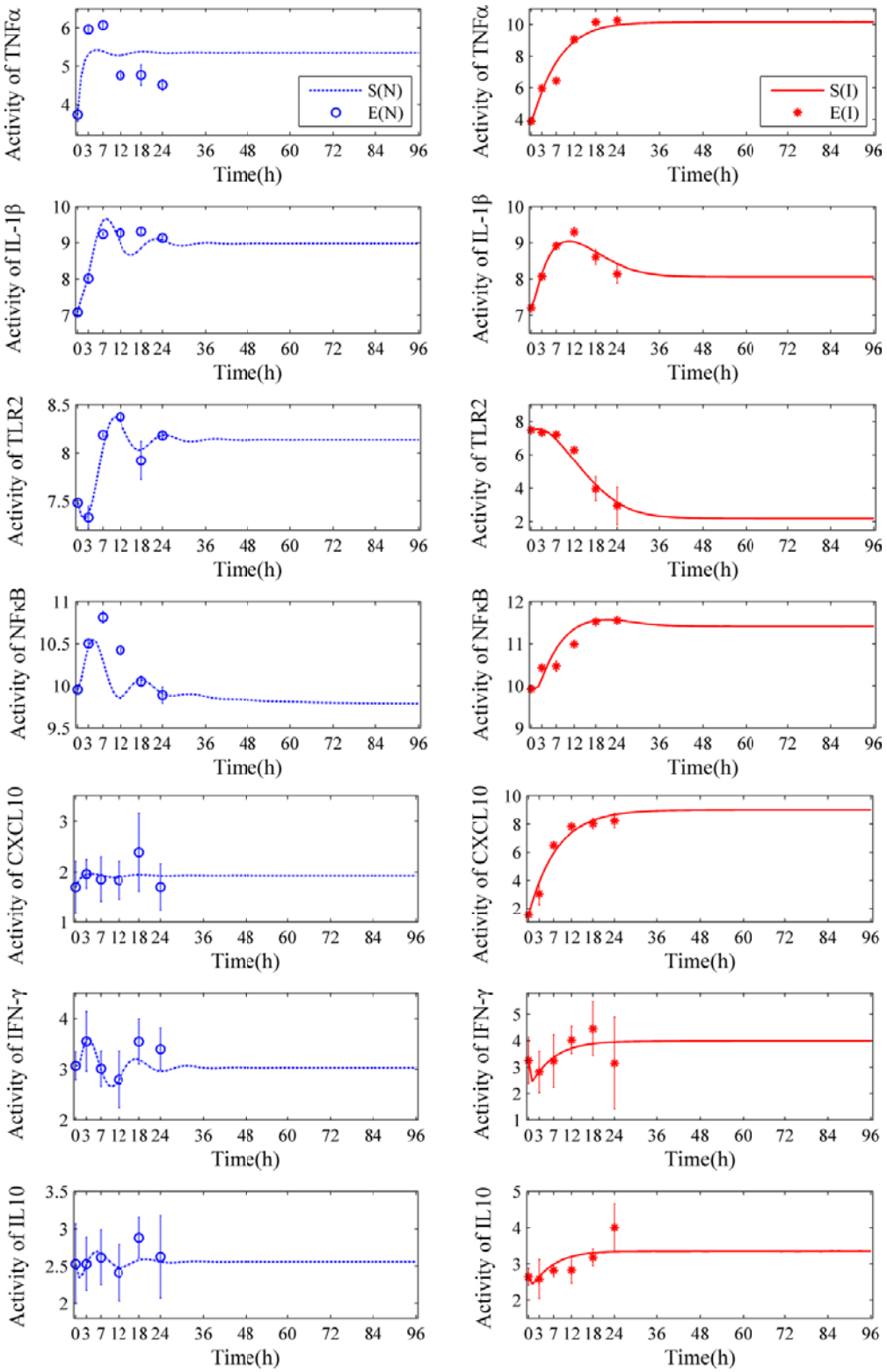


**Figure S9 | Dynamical process of TNFα, IL-1β, TLR2, NFκB, CXCL10, IFN-γ and IL10 in the normal network (N) and the inflammatory network (I) over 96h.** The blue dashed and red solid lines denote the simulation results (S) of the normal and inflammatory networks, respectively. The blue circle and red stars represent the experimental data (E) at each time point of the normal and inflammatory network, respectively. The experimental errors are plotted using short bars at each time point.

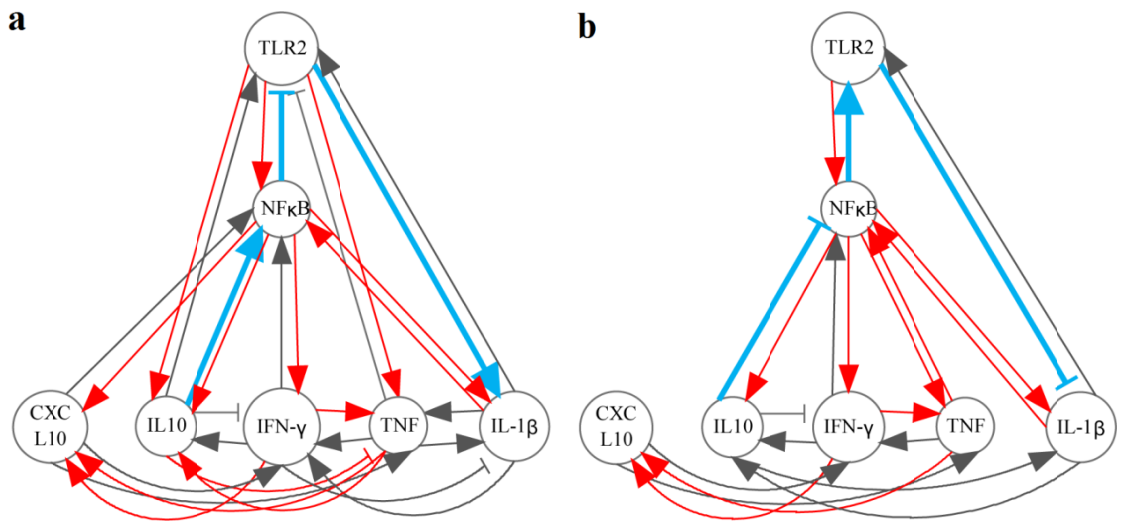


**Figure S10 | Network structures derived from the dynamical models.** The gray lines indicate the regulatory interactions predicted by our models. The red lines represent the regulatory interactions confirmed in the literature. The blue thick lines stand for the opposite regulatory interactions predicted by our models (comparison of two networks). The lines with arrows and short bars indicate positive and negative regulation, respectively. (a) Predicted by the inflammatory network model. (b) Predicted by the normal network model.

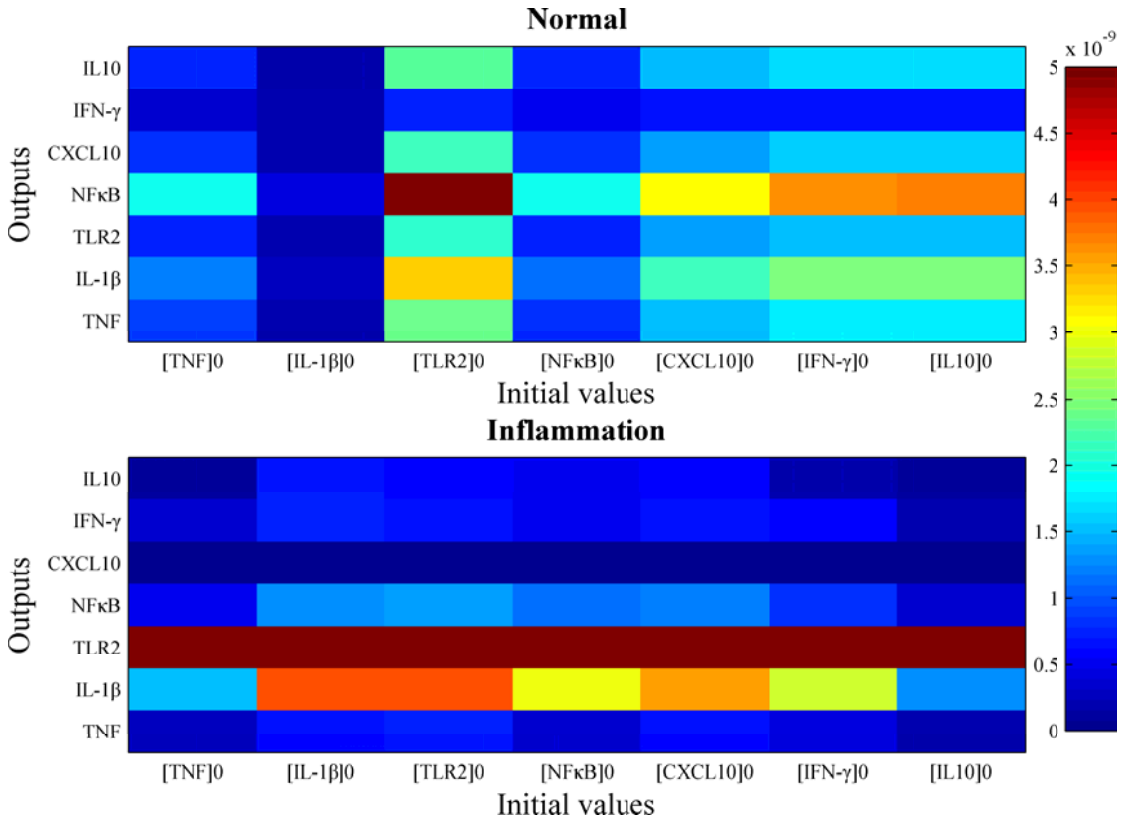


**Figure S11 | Local robustness (LR) with respect to the initial values in the normal and inflammatory networks with 10% perturbations.** [X]0 is the initial value of the output X in the dynamical models. The results show that both networks are very robust to perturbations of the initial concentrations of proteins.

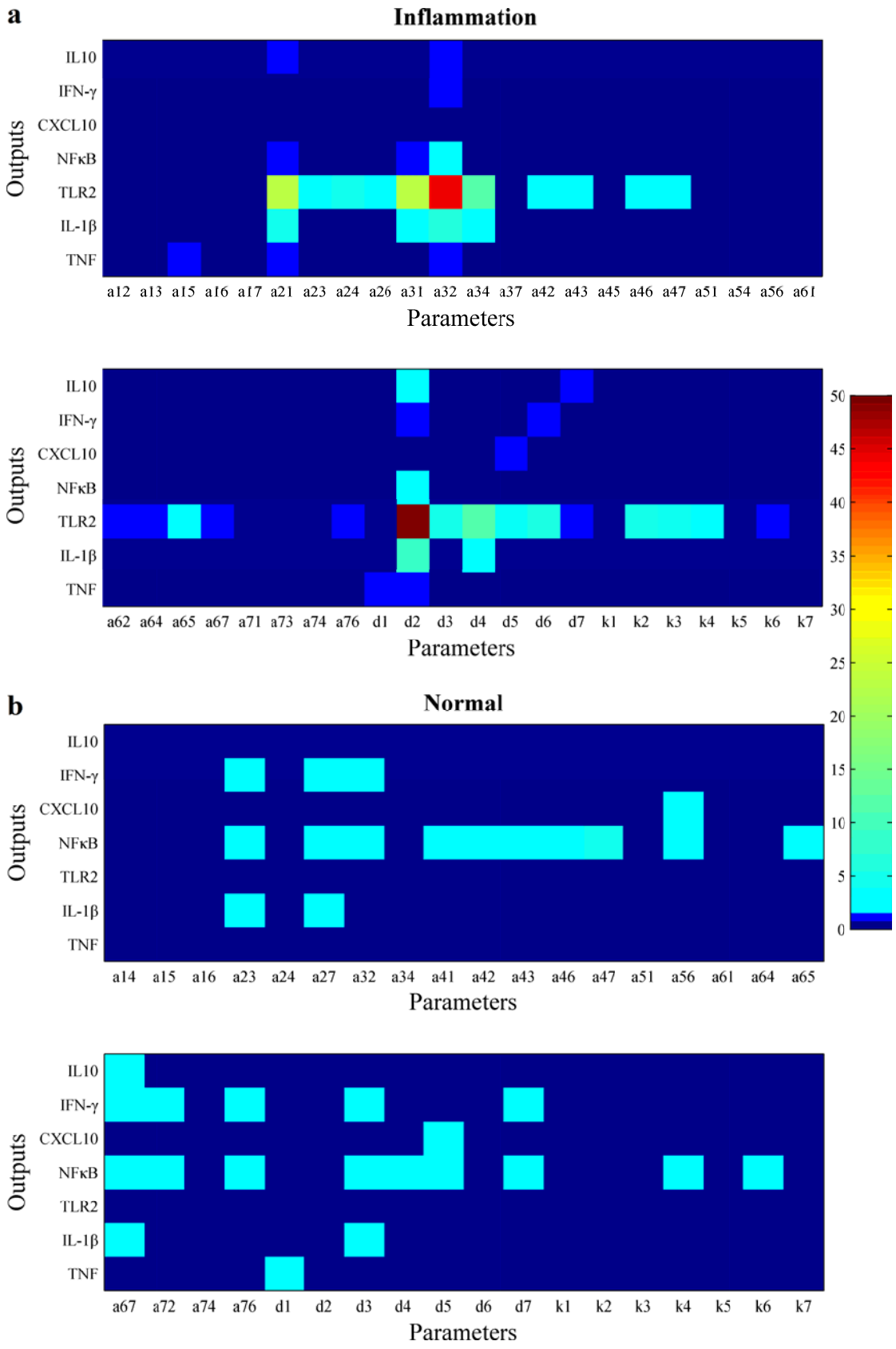


**Figure S12 | Local robustness (LR) with respect to the kinetic parameters with 10% perturbations.** The blue color in the color bar indicates values that are less than 0.6. (a) Normal network. (b) Inflammatory network.

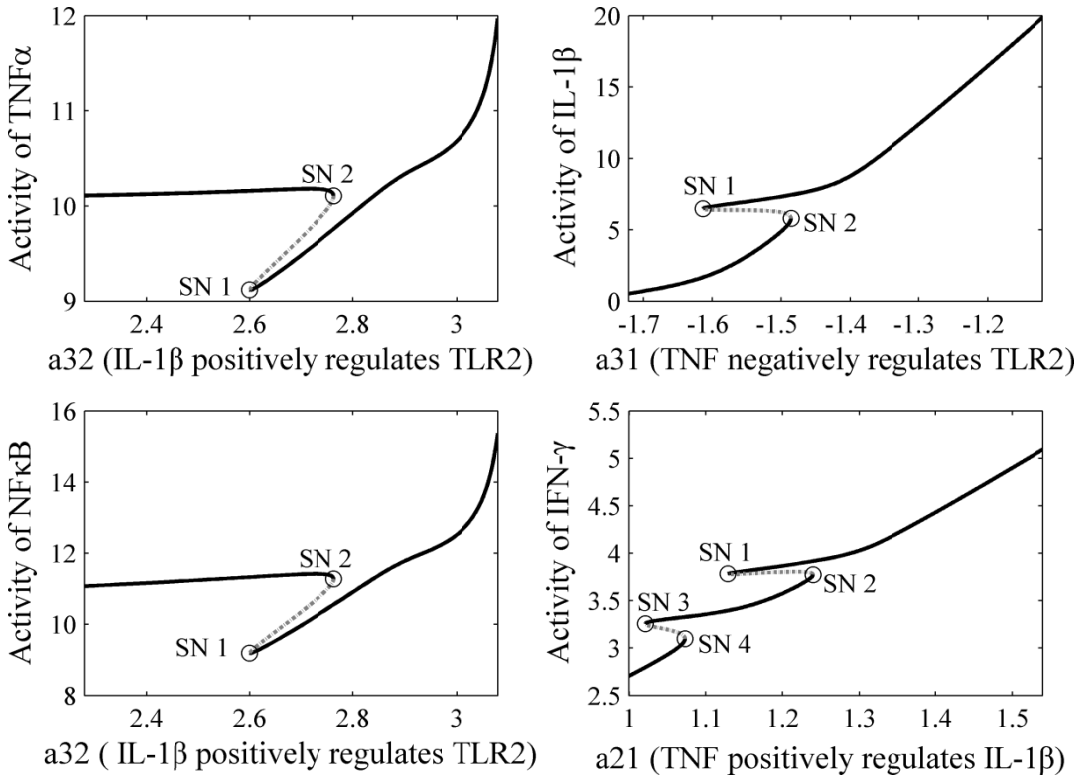


**Figure S13 | Bistability and tristability phenomena for sensitive parameters a32, a31 and a21 in the inflammatory network.** SN represents a saddle-node bifurcation.

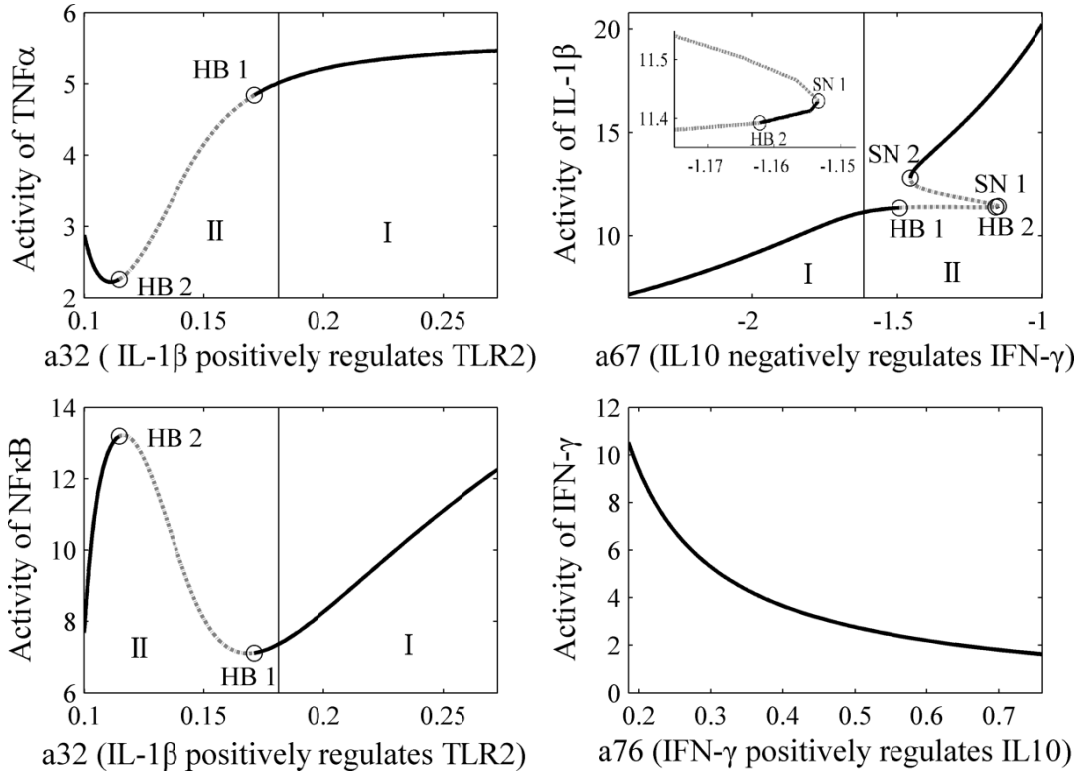


**Figure S14 | Bifurcation graph for the sensitive parameters a32, a67 and a76 in the normal network.** HB and SN represent a Hopf bifurcation and a saddle-node bifurcation, respectively. Domain I is the parameter range for the 20% perturbation. Domain II exhibits an HB and oscillation.

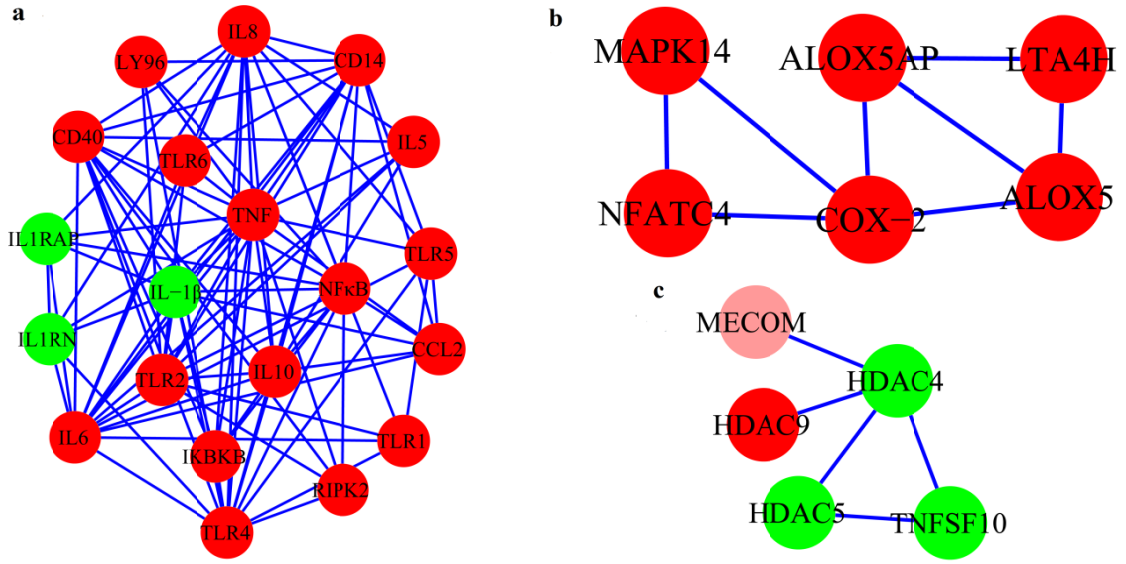


**Figure S15 | Three related modules in the inflammatory network identified using the Cytoscape plugin ClusterOne.** The red and green colors indicate the increased and decreased entropy of the proteins, respectively. (a) Module including TNF, IL-1β, TLR2, NFκB, and IL10. (b) Module of COX-2. (c) Module of the protein complex (TNFSF10/HDAC4/HDAC5).

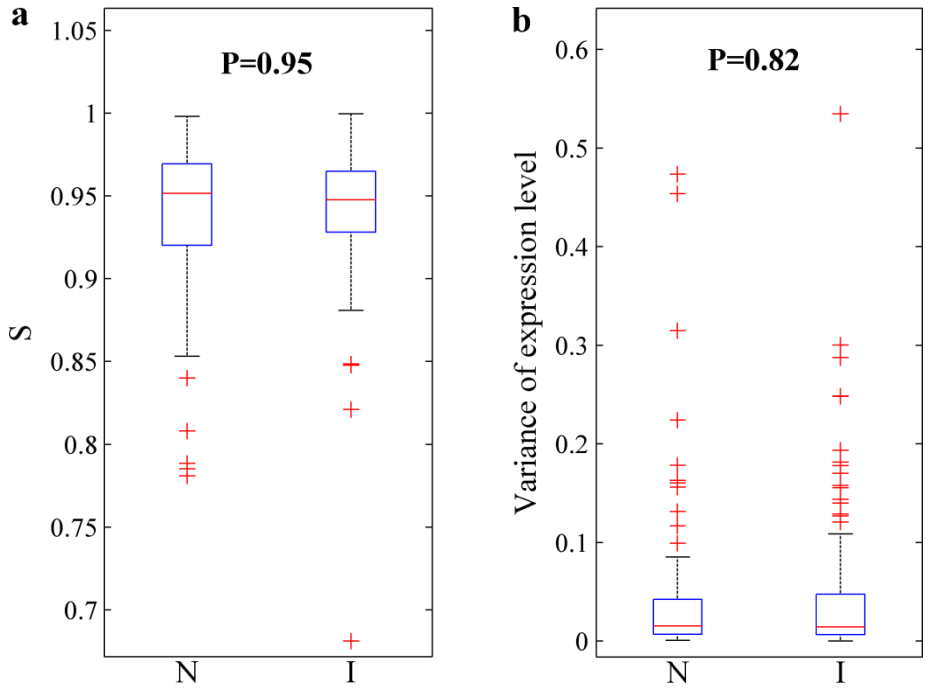


**Figure S16 | Comparison of the local network entropies (S) and the variance of protein expression levels between the inflammatory (I) and normal networks (N) for HCV infection.** P-values are from a two-tailed Wilcoxon rank sum test. (a) Comparison of the local network entropies for all nodes with degree ≥2. (b) Comparison of the variance of protein expression levels for all nodes. There are not significant differences in both the entropies and the variance of protein expression levels between the normal and inflammatory networks for HCV infection.

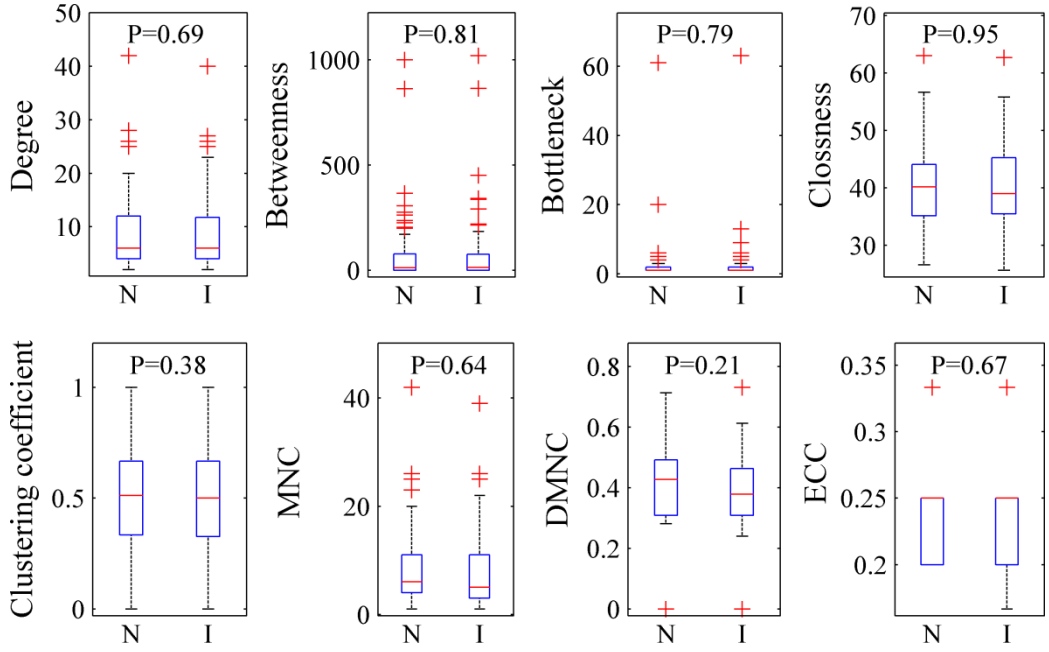


**Figure S17 | Comparison between the inflammatory (I) and normal (N) networks of eight local network metrics for all nodes with degree ≥2 for HCV infection.** P-values are from a two-tailed Wilcoxon rank sum test.

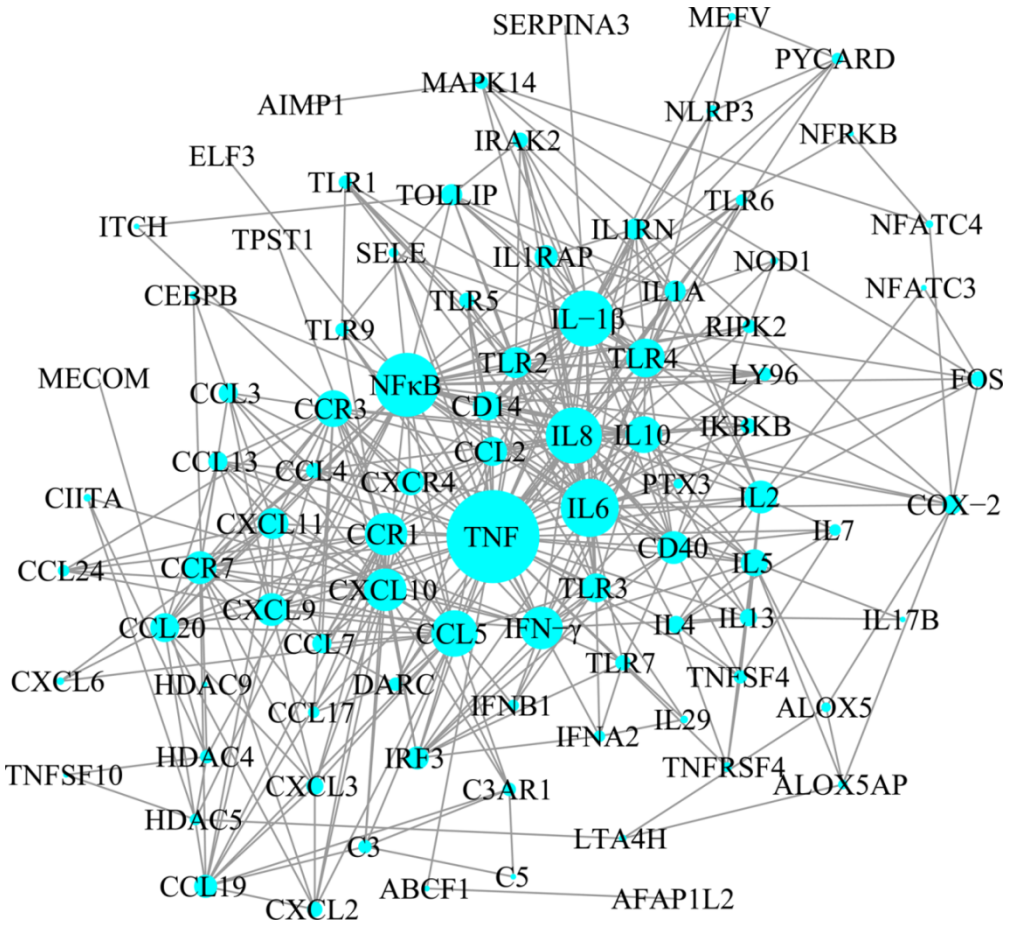


**Figure S18 | PPI network collected from four PPI databases (BIND, HPRD, BioGRID and STRING).** The node sizes are proportional to the degree of the nodes.

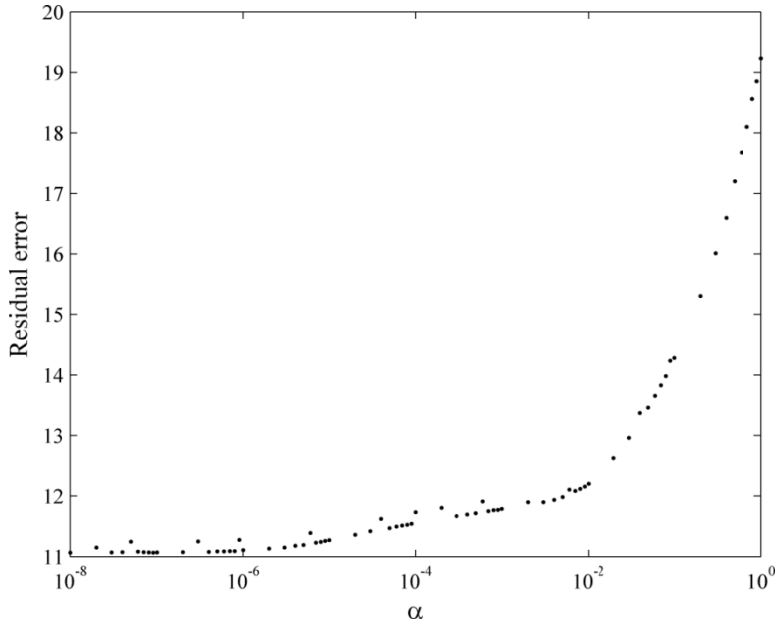


**Figure S19 | Residual error of the inflammatory network model for various values of the constant *α*.**

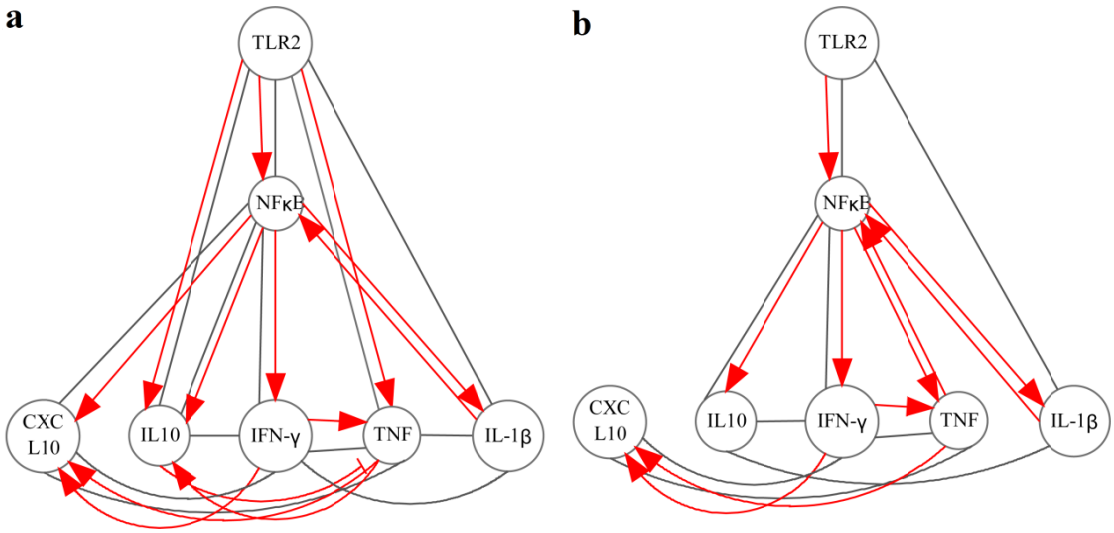


**Figure S20 | Interactions of these potential target proteins in the constructed inflammatory network (a) and normal network (b) are shown, respectively.** The gray lines indicate the interactions in the constructed networks. The red lines represent the regulatory interactions confirmed in the literatures. The lines with arrows and short bars indicate positive and negative regulations, respectively.

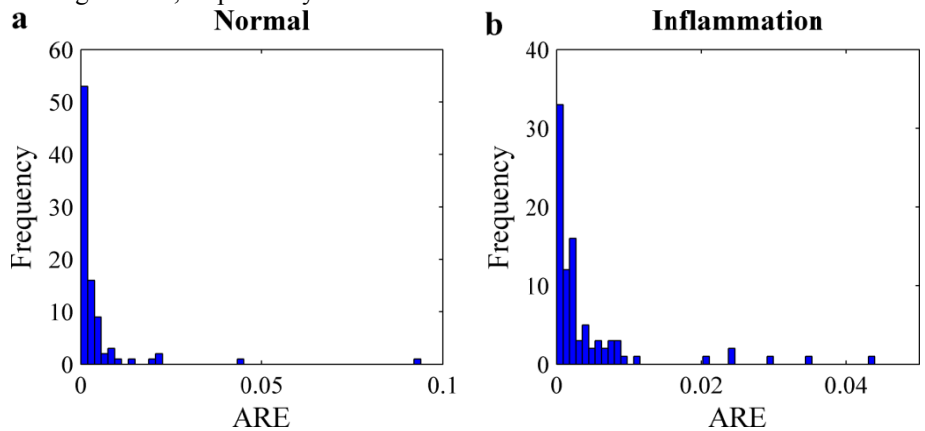


**Figure S21 | Average relative errors (AREs) of the networks.** The y-axis represents the number of nodes in networks whose AREs are fall into the corresponding bins. (a) and (b) are the distributions of the AREs of the normal and inflammatory networks for HCV infection, respectively.

## Supplementary Tables:

**Table S1 | Detailed global topological metrics of the inflammatory and normal networks for the H5N1 and H1N1 infections**

| topological metrics | H5N1 | | H1N1 | |
|---|---|---|---|---|
| | inflammatory network | normal network | inflammatory network | normal network |
| network diameter | 6 | 6 | 6 | 6 |
| network density | 0.098 | 0.094 | 0.099 | 0.092 |
| network centralization | 0.417 | 0.387 | 0.363 | 0.306 |
| average path-length | 2.545 | 2.573 | 2.541 | 2.569 |
| average number of neighbors | 8.733 | 8.136 | 8.483 | 8.0 |
| average clustering coefficient | 0.520 | 0.454 | 0.496 | 0.478 |

**Table S2 | Optimal parameter values obtained by DMGBDE algorithm in the inflammatory network model**

| Kinetic parameter | Biological process | Optimal value | Kinetic parameter | Biological process | Optimal value |
|---|---|---|---|---|---|
| a12 | IL-1β→TNFα | 0.0776 | a62 | IL-1β→IFN-γ | 0.3130 |
| a13 | TLR2→TNFα | 2.5419 | a64 | NFκB→IFN-γ | 2.7954 |
| a15 | CXCL10→TNFα | 1.8110 | a65 | CXCL10→IFN-γ | 0.6673 |
| a16 | IFN-γ→TNFα | 2.5771 | a67 | IL10—\|IFN-γ | -0.6650 |
| a17 | IL10—\|TNFα | -2.5470 | a71 | TNFα→IL10 | 1.4850 |
| a21 | TNFα→IL-1β | 1.2849 | a73 | TLR2→IL10 | 1.1734 |
| a23 | TLR2→IL-1β | 1.0904 | a74 | NFκB→IL10 | 1.5965 |
| a24 | NFκB→IL-1β | 2.4924 | a76 | IFN-γ→IL10 | 3.5223 |
| a26 | IFN-γ—\|IL-1β | -0.3075 | d1 | TNFα degradation | 2.1500 |
| a31 | TNFα—\|TLR2 | -1.4332 | d2 | IL-1β degradation | 2.3792 |
| a32 | IL-1β→TLR2 | 2.8533 | d3 | TLR2 degradation | 1.3920 |
| a34 | NFκB—\|TLR2 | -0.6967 | d4 | NFκB degradation | 1.4283 |
| a37 | IL10→TLR2 | 0.0839 | d5 | CXCL10 degradation | 0.1317 |
| a42 | IL-1β→NFκB | 3.0824 | d6 | IFN-γ degradation | 3.2306 |
| a43 | TLR2→NFκB | 3.3122 | d7 | IL10 degradation | 5.8791 |
| a45 | CXCL10→NFκB | 0.1011 | k1 | TNFα synthesis | 2.7397 |
| a46 | IFN-γ→NFκB | 0.6207 | k2 | IL-1β synthesis | 2.4806 |
| a47 | IL10→NFκB | 1.2172 | k3 | TLR2 synthesis | 2.2888 |
| a51 | TNFα→CXCL10 | 0.2873 | k4 | NFκB synthesis | 3.0622 |
| a54 | NFκB→CXCL10 | 0.3028 | k5 | CXCL10 synthesis | 0.2603 |
| a56 | IFN-γ→CXCL10 | 0.3604 | k6 | IFN-γ synthesis | 2.3243 |
| a61 | TNFα→IFN-γ | 0.1475 | k7 | IL10 synthesis | 1.5914 |

**Table S3 | Optimal parameter values obtained by DMGBDE algorithm in normal network model**

| Kinetic parameter | Biological process | Optimal value | Kinetic parameter | Biological process | Optimal value |
|---|---|---|---|---|---|
| a14 | NFκB→TNFα | 0.8388 | a67 | IL10—\|IFN-γ | -2.022 |
| a15 | CXCL10→TNFα | 1.3521 | a72 | IL-1β→IL10 | 0.2335 |
| a16 | IFN-γ→TNFα | 1.8693 | a74 | NFκB→IL10 | 0.0473 |
| a23 | TLR2—\|IL-1β | -0.508 | a76 | IFN-γ→IL10 | 0.4647 |
| a24 | NFκB→IL-1β | 0.7257 | d1 | TNFα degradation | 1.1549 |
| a27 | IL10→IL-1β | 1.4590 | d2 | IL-1β degradation | 0.1256 |
| a32 | IL-1β→TLR2 | 0.2264 | d3 | TLR2 degradation | 0.3387 |
| a34 | NFκB→TLR2 | 0.0220 | d4 | NFκB degradation | 0.0557 |
| a41 | TNFα→NFκB | 0.6108 | d5 | CXCL10 degradation | 1.1194 |
| a42 | IL-1β→NFκB | 0.6353 | d6 | IFN-γ degradation | 0.0154 |
| a43 | TLR2→NFκB | 0.6600 | d7 | IL10 degradation | 1.4093 |
| a46 | IFN-γ→NFκB | 0.2391 | k1 | TNFα synthesis | 1.0607 |
| a47 | IL10—\|NFκB | -0.9893 | k2 | IL-1β synthesis | 0.8100 |
| a51 | TNFα→CXCL10 | 0.098 | k3 | TLR2 synthesis | 0.5081 |
| a56 | IFN-γ→CXCL10 | 1.7629 | k4 | NFκB synthesis | 0.4845 |
| a61 | TNFα→IFN-γ | 0.1242 | k5 | CXCL10 synthesis | 0.4727 |
| a64 | NFκB→IFN-γ | 1.0415 | k6 | IFN-γ synthesis | 1.2469 |
| a65 | CXCL10→IFN-γ | 1.1820 | k7 | IL10 synthesis | 0.0548 |

**Table S4. Local robustness analysis of the initial values in the normal network model with 5% perturbations**

| Initial values | Robustness measure $LR_i$ with respect to different outputs | | | | | | |
|---|---|---|---|---|---|---|---|
| | TNFα | IL-1β | TLR2 | NFκB | CXCL10 | IFN-γ | IL10 |
| $[TNF\alpha]_0$ | 1.24E-09 | 1.83E-09 | 1.09E-09 | 2.83E-09 | 1.11E-09 | 5.44E-10 | 1.19E-09 |
| $[IL\text{-}1\beta]_0$ | 2.01E-10 | 3.65E-10 | 1.25E-10 | 9.32E-10 | 1.28E-10 | 1.04E-10 | 1.58E-10 |
| $[TLR2]_0$ | 3.98E-09 | 5.53E-09 | 3.47E-09 | 8.11E-09 | 3.56E-09 | 1.39E-09 | 3.81E-09 |
| $[NF\kappa B]_0$ | 1.20E-09 | 1.74E-09 | 1.05E-09 | 2.62E-09 | 1.12E-09 | 4.57E-10 | 1.15E-09 |
| $[CXCL10]_0$ | 2.50E-09 | 3.64E-09 | 2.22E-09 | 5.43E-09 | 2.27E-09 | 8.89E-10 | 2.43E-09 |
| $[IFN\text{-}\gamma]_0$ | 2.93E-09 | 4.04E-09 | 2.56E-09 | 5.79E-09 | 2.60E-09 | 1.10E-09 | 2.80E-09 |
| $[IL10]_0$ | 2.98E-09 | 4.14E-09 | 2.60E-09 | 6.35E-09 | 2.66E-09 | 1.05E-09 | 2.84E-09 |

Note: $[X]_0$ indicates the initial value of protein X in the dynamical models.

**Table S5. Local robustness analysis of the initial values in the normal network model with 10% perturbations**

| Initial values | Robustness measure $LR_i$ with respect to different outputs | | | | | | |
|---|---|---|---|---|---|---|---|
| | TNFα | IL-1β | TLR2 | NFκB | CXCL10 | IFN-γ | IL10 |
| $[TNF\alpha]_0$ | 9.00E-10 | 1.23E-09 | 7.73E-10 | 1.93E-09 | 7.92E-10 | 3.38E-10 | 8.41E-10 |
| $[IL\text{-}1\beta]_0$ | 2.15E-10 | 2.79E-10 | 1.88E-10 | 4.64E-10 | 2.01E-10 | 1.91E-10 | 2.06E-10 |
| $[TLR2]_0$ | 2.38E-09 | 3.34E-09 | 2.09E-09 | 4.94E-09 | 2.13E-09 | 7.69E-10 | 2.29E-09 |
| $[NF\kappa B]_0$ | 8.57E-10 | 1.17E-09 | 7.25E-10 | 1.94E-09 | 7.93E-10 | 4.69E-10 | 7.89E-10 |
| $[CXCL10]_0$ | 1.56E-09 | 2.16E-09 | 1.36E-09 | 3.10E-09 | 1.39E-09 | 6.30E-10 | 1.50E-09 |
| $[IFN\text{-}\gamma]_0$ | 1.78E-09 | 2.46E-09 | 1.54E-09 | 3.62E-09 | 1.58E-09 | 6.97E-10 | 1.71E-09 |
| $[IL10]_0$ | 1.75E-09 | 2.47E-09 | 1.53E-09 | 3.69E-09 | 1.59E-09 | 6.69E-10 | 1.71E-09 |

Note: $[X]_0$ indicates the initial value of protein X in the dynamical models.

**Table S6. Local robustness analysis of initial values in normal network model with 20% perturbations**

| Initial values | Robustness measure $LR_i$ with respect to different outputs | | | | | | |
|---|---|---|---|---|---|---|---|
| | TNFα | IL-1β | TLR2 | NFκB | CXCL10 | IFN-γ | IL10 |
| $[TNF\alpha]_0$ | 5.67E-10 | 7.97E-10 | 4.99E-10 | 1.14E-09 | 5.16E-10 | 1.88E-10 | 5.49E-10 |
| $[IL\text{-}1\beta]_0$ | 1.55E-10 | 2.12E-10 | 1.32E-10 | 3.04E-10 | 1.40E-10 | 5.79E-11 | 1.47E-10 |
| $[TLR2]_0$ | 1.08E-09 | 1.54E-09 | 9.63E-10 | 2.19E-09 | 9.79E-10 | 3.43E-10 | 1.06E-09 |
| $[NF\kappa B]_0$ | 4.92E-10 | 6.72E-10 | 4.19E-10 | 9.83E-10 | 4.57E-10 | 1.76E-10 | 4.68E-10 |
| $[CXCL10]_0$ | 1.02E-09 | 1.44E-09 | 9.00E-10 | 2.04E-09 | 9.18E-10 | 3.29E-10 | 9.89E-10 |
| $[IFN\text{-}\gamma]_0$ | 1.07E-09 | 1.51E-09 | 9.46E-10 | 2.15E-09 | 9.66E-10 | 3.44E-10 | 1.04E-09 |
| $[IL10]_0$ | 9.03E-10 | 1.26E-09 | 7.93E-10 | 1.79E-09 | 8.23E-10 | 3.02E-10 | 8.74E-10 |

Note: $[X]_0$ indicates the initial value of protein X in the dynamical models.

**Table S7. Local robustness analysis of initial values in inflammatory network model with 5% perturbations**

| Initial values | Robustness measure $LR_i$ with respect to different outputs | | | | | | |
|---|---|---|---|---|---|---|---|
| | TNFα | IL-1β | TLR2 | NFκB | CXCL10 | IFN-γ | IL10 |
| $[TNF\alpha]_0$ | 1.39E-09 | 6.86E-09 | 4.60E-08 | 2.16E-09 | 6.69E-11 | 1.26E-09 | 1.19E-09 |
| $[IL\text{-}1\beta]_0$ | 1.13E-09 | 6.98E-09 | 5.33E-08 | 2.27E-09 | 7.14E-11 | 1.25E-09 | 1.20E-09 |
| $[TLR2]_0$ | 9.03E-10 | 2.81E-09 | 2.65E-08 | 7.84E-10 | 4.19E-11 | 5.72E-10 | 7.22E-10 |
| $[NF\kappa B]_0$ | 7.28E-10 | 2.39E-09 | 2.13E-08 | 8.85E-10 | 1.70E-11 | 3.78E-10 | 3.89E-10 |
| $[CXCL10]_0$ | 1.23E-09 | 6.30E-09 | 4.20E-08 | 2.15E-09 | 1.05E-10 | 1.19E-09 | 5.87E-10 |
| $[IFN\text{-}\gamma]_0$ | 6.65E-10 | 4.49E-09 | 3.87E-08 | 1.18E-09 | 5.25E-11 | 8.21E-10 | 6.59E-10 |
| $[IL10]_0$ | 1.17E-09 | 5.44E-09 | 3.47E-08 | 1.95E-09 | 1.49E-10 | 1.01E-09 | 5.10E-10 |

Note: $[X]_0$ indicates the initial value of protein X in the dynamical models.

**Table S8. Local robustness analysis of the initial values in inflammatory network model with 10% perturbations**

| Initial values | Robustness measure $LR_i$ with respect to different outputs | | | | | | |
|---|---|---|---|---|---|---|---|
| | TNFα | IL-1β | TLR2 | NFκB | CXCL10 | IFN-γ | IL10 |
| $[TNF\alpha]_0$ | 2.53E-10 | 1.55E-09 | 1.36E-08 | 4.83E-10 | 2.02E-11 | 3.17E-10 | 1.51E-10 |
| $[IL\text{-}1\beta]_0$ | 6.79E-10 | 3.96E-09 | 2.97E-08 | 1.31E-09 | 4.78E-11 | 7.05E-10 | 7.10E-10 |
| $[TLR2]_0$ | 7.44E-10 | 3.97E-09 | 2.77E-08 | 1.33E-09 | 5.50E-11 | 6.84E-10 | 5.90E-10 |
| $[NF\kappa B]_0$ | 3.40E-10 | 3.03E-09 | 2.21E-08 | 1.13E-09 | 4.58E-11 | 5.00E-10 | 5.09E-10 |
| $[CXCL10]_0$ | 6.85E-10 | 3.53E-09 | 2.47E-08 | 1.24E-09 | 7.17E-11 | 6.65E-10 | 5.60E-10 |
| $[IFN\text{-}\gamma]_0$ | 4.35E-10 | 2.84E-09 | 2.33E-08 | 8.04E-10 | 1.92E-11 | 5.59E-10 | 2.00E-10 |
| $[IL10]_0$ | 2.25E-10 | 1.32E-09 | 1.08E-08 | 3.79E-10 | 1.93E-11 | 2.16E-10 | 1.16E-10 |

Note: $[X]_0$ indicates the initial value of protein X in the dynamical models.

**Table S9. Local robustness analysis of the initial values in inflammatory network model with 20% perturbations**

| Initial values | Robustness measure $LR_i$ with respect to different outputs | | | | | | |
|---|---|---|---|---|---|---|---|
| | TNFα | IL-1β | TLR2 | NFκB | CXCL10 | IFN-γ | IL10 |
| $[TNF\alpha]_0$ | 1.19E-10 | 8.27E-10 | 7.29E-09 | 2.21E-10 | 6.30E-12 | 1.45E-10 | 4.16E-11 |
| $[IL\text{-}1\beta]_0$ | 1.72E-10 | 1.29E-09 | 1.14E-08 | 3.11E-10 | 7.29E-12 | 2.27E-10 | 5.47E-11 |
| $[TLR2]_0$ | 1.15E-10 | 8.21E-10 | 7.18E-09 | 2.10E-10 | 5.27E-12 | 1.43E-10 | 4.03E-11 |
| $[NF\kappa B]_0$ | 1.10E-10 | 7.75E-10 | 6.69E-09 | 2.03E-10 | 5.38E-12 | 1.37E-10 | 4.29E-11 |
| $[CXCL10]_0$ | 1.58E-10 | 1.10E-09 | 9.73E-09 | 2.95E-10 | 5.79E-12 | 1.93E-10 | 5.20E-11 |

| | | | | | | | |
|---|---|---|---|---|---|---|---|
| $[IFN\text{-}\gamma]_0$ | 1.78E-10 | 1.33E-09 | 1.17E-08 | 3.38E-10 | 7.33E-12 | 2.32E-10 | 5.55E-11 |
| $[IL10]_0$ | 9.06E-11 | 6.21E-10 | 5.36E-09 | 1.60E-10 | 4.92E-12 | 1.10E-10 | 3.71E-11 |

Note: $[X]_0$ indicates the initial value of protein X in the dynamical models.

**Table S10. Local robustness analysis of kinetic parameters in the normal network model with 5% perturbations**

| Parameters | Robustness measure $LR_i$ with respect to different outputs | | | | | | |
|---|---|---|---|---|---|---|---|
| | TNFα | IL-1β | TLR2 | NFκB | CXCL10 | IFN-γ | IL10 |
| a14 | 0.136 | 0.020 | 0.011 | 0.052 | 0.003 | 0.017 | 0.018 |
| a15 | 0.428 | 0.064 | 0.034 | 0.163 | 0.009 | 0.053 | 0.058 |
| a16 | 0.277 | 0.041 | 0.022 | 0.106 | 0.006 | 0.034 | 0.037 |
| a23 | 0.217 | 0.999 | 0.598 | 1.773 | 0.268 | 1.837 | 0.136 |
| a24 | 0.037 | 0.174 | 0.104 | 0.308 | 0.046 | 0.319 | 0.024 |
| a27 | 0.195 | 0.902 | 0.540 | 1.602 | 0.241 | 1.658 | 0.123 |
| a32 | 0.160 | 0.739 | 0.298 | 1.337 | 0.198 | 1.359 | 0.101 |
| a34 | 0.017 | 0.078 | 0.031 | 0.142 | 0.021 | 0.144 | 0.011 |
| a41 | 0.021 | 0.075 | 0.039 | 1.211 | 0.022 | 0.152 | 0.016 |
| a42 | 0.022 | 0.080 | 0.042 | 1.287 | 0.023 | 0.162 | 0.017 |
| a43 | 0.023 | 0.083 | 0.043 | 1.334 | 0.024 | 0.167 | 0.018 |
| a46 | 0.026 | 0.092 | 0.048 | 1.485 | 0.027 | 0.186 | 0.020 |
| a47 | 0.089 | 0.321 | 0.168 | 5.192 | 0.095 | 0.651 | 0.069 |
| a51 | 0.021 | 0.026 | 0.013 | 0.077 | 0.047 | 0.020 | 0.023 |
| a56 | 0.345 | 0.437 | 0.221 | 1.291 | 0.786 | 0.329 | 0.382 |
| a61 | 0.012 | 0.154 | 0.078 | 0.464 | 0.017 | 0.115 | 0.134 |
| a64 | 0.018 | 0.239 | 0.120 | 0.719 | 0.026 | 0.178 | 0.208 |
| a65 | 0.041 | 0.529 | 0.266 | 1.588 | 0.057 | 0.393 | 0.461 |
| a67 | 0.092 | 1.202 | 0.604 | 3.610 | 0.130 | 0.894 | 1.047 |
| a72 | 0.219 | 0.013 | 0.135 | 1.853 | 0.270 | 1.862 | 0.138 |
| a74 | 0.005 | 0.000 | 0.003 | 0.041 | 0.006 | 0.042 | 0.003 |
| a76 | 0.147 | 0.009 | 0.091 | 1.245 | 0.182 | 1.251 | 0.093 |
| d1 | 1.016 | 0.151 | 0.081 | 0.388 | 0.021 | 0.126 | 0.137 |
| d2 | 0.059 | 0.273 | 0.163 | 0.484 | 0.073 | 0.501 | 0.037 |
| d3 | 0.216 | 1.002 | 0.403 | 1.814 | 0.267 | 1.841 | 0.136 |
| d4 | 0.019 | 0.069 | 0.036 | 1.120 | 0.020 | 0.141 | 0.015 |
| d5 | 0.469 | 0.593 | 0.300 | 1.753 | 1.067 | 0.447 | 0.519 |
| d6 | 0.001 | 0.011 | 0.005 | 0.033 | 0.001 | 0.008 | 0.009 |
| d7 | 0.379 | 0.024 | 0.233 | 3.179 | 0.468 | 3.203 | 0.239 |
| k1 | 0.174 | 0.026 | 0.014 | 0.066 | 0.004 | 0.022 | 0.024 |
| k2 | 0.042 | 0.196 | 0.117 | 0.348 | 0.052 | 0.360 | 0.027 |
| k3 | 0.040 | 0.185 | 0.074 | 0.334 | 0.049 | 0.339 | 0.025 |
| k4 | 0.017 | 0.062 | 0.032 | 0.994 | 0.018 | 0.125 | 0.013 |
| k5 | 0.103 | 0.130 | 0.066 | 0.384 | 0.234 | 0.098 | 0.114 |
| k6 | 0.022 | 0.290 | 0.146 | 0.870 | 0.031 | 0.215 | 0.252 |
| k7 | 0.006 | 0.000 | 0.004 | 0.048 | 0.007 | 0.049 | 0.004 |

Note: Larger values are marked in red.

**Table S11. Local robustness analysis of kinetic parameters in the normal network model with 10% perturbations**

| Parameters | Robustness measure $LR_i$ with respect to different outputs | | | | | | |
|---|---|---|---|---|---|---|---|
| | TNFα | IL-1β | TLR2 | NFκB | CXCL10 | IFN-γ | IL10 |
| a14 | 0.136 | 0.020 | 0.011 | 0.052 | 0.003 | 0.017 | 0.018 |
| a15 | 0.428 | 0.064 | 0.034 | 0.163 | 0.009 | 0.053 | 0.058 |
| a16 | 0.277 | 0.041 | 0.022 | 0.106 | 0.006 | 0.034 | 0.037 |
| a23 | 0.217 | 0.997 | 0.597 | 1.770 | 0.268 | 1.835 | 0.137 |
| a24 | 0.038 | 0.174 | 0.104 | 0.308 | 0.046 | 0.319 | 0.024 |
| a27 | 0.196 | 0.901 | 0.540 | 1.598 | 0.243 | 1.658 | 0.124 |
| a32 | 0.160 | 0.738 | 0.297 | 1.335 | 0.198 | 1.357 | 0.101 |
| a34 | 0.017 | 0.078 | 0.031 | 0.142 | 0.021 | 0.144 | 0.011 |
| a41 | 0.021 | 0.075 | 0.039 | 1.211 | 0.022 | 0.152 | 0.016 |
| a42 | 0.022 | 0.080 | 0.042 | 1.287 | 0.023 | 0.162 | 0.017 |
| a43 | 0.023 | 0.083 | 0.043 | 1.334 | 0.024 | 0.167 | 0.018 |
| a46 | 0.026 | 0.092 | 0.048 | 1.486 | 0.027 | 0.186 | 0.020 |
| a47 | 0.090 | 0.319 | 0.170 | 5.183 | 0.095 | 0.650 | 0.070 |
| a51 | 0.021 | 0.026 | 0.013 | 0.077 | 0.047 | 0.020 | 0.023 |
| a56 | 0.345 | 0.437 | 0.221 | 1.291 | 0.786 | 0.329 | 0.382 |
| a61 | 0.012 | 0.154 | 0.078 | 0.464 | 0.017 | 0.115 | 0.134 |
| a64 | 0.018 | 0.239 | 0.120 | 0.719 | 0.026 | 0.178 | 0.208 |
| a65 | 0.041 | 0.529 | 0.266 | 1.588 | 0.057 | 0.393 | 0.460 |
| a67 | 0.092 | 1.200 | 0.603 | 3.604 | 0.130 | 0.893 | 1.045 |
| a72 | 0.221 | 0.016 | 0.136 | 1.847 | 0.273 | 1.863 | 0.139 |
| a74 | 0.005 | 0.000 | 0.003 | 0.041 | 0.006 | 0.042 | 0.003 |
| a76 | 0.147 | 0.009 | 0.091 | 1.243 | 0.182 | 1.249 | 0.093 |
| d1 | 1.014 | 0.151 | 0.081 | 0.387 | 0.021 | 0.126 | 0.137 |
| d2 | 0.059 | 0.272 | 0.163 | 0.484 | 0.073 | 0.501 | 0.037 |
| d3 | 0.218 | 1.000 | 0.403 | 1.808 | 0.269 | 1.841 | 0.137 |
| d4 | 0.019 | 0.069 | 0.036 | 1.118 | 0.020 | 0.140 | 0.015 |
| d5 | 0.468 | 0.592 | 0.300 | 1.751 | 1.066 | 0.446 | 0.518 |
| d6 | 0.001 | 0.011 | 0.005 | 0.033 | 0.001 | 0.008 | 0.009 |
| d7 | 0.380 | 0.040 | 0.233 | 3.176 | 0.469 | 3.202 | 0.240 |
| k1 | 0.174 | 0.026 | 0.014 | 0.066 | 0.004 | 0.022 | 0.024 |
| k2 | 0.042 | 0.196 | 0.117 | 0.347 | 0.052 | 0.360 | 0.027 |
| k3 | 0.040 | 0.185 | 0.074 | 0.334 | 0.049 | 0.339 | 0.025 |
| k4 | 0.017 | 0.062 | 0.032 | 0.994 | 0.018 | 0.125 | 0.013 |
| k5 | 0.103 | 0.130 | 0.066 | 0.384 | 0.234 | 0.098 | 0.114 |
| k6 | 0.022 | 0.289 | 0.146 | 0.870 | 0.031 | 0.215 | 0.252 |
| k7 | 0.006 | 0.000 | 0.004 | 0.048 | 0.007 | 0.049 | 0.004 |

Note: Larger values are marked in red.

**Table S12. Local robustness analysis of kinetic parameters in the normal network model with 20% perturbations**

| Parameters | Robustness measure $LR_i$ with respect to different outputs | | | | | | |
|---|---|---|---|---|---|---|---|
| | TNFα | IL-1β | TLR2 | NFκB | CXCL10 | IFN-γ | IL10 |
| a14 | 0.139 | 0.021 | 0.011 | 0.053 | 0.003 | 0.017 | 0.019 |
| a15 | 0.435 | 0.065 | 0.035 | 0.166 | 0.009 | 0.054 | 0.059 |
| a16 | 0.282 | 0.042 | 0.023 | 0.107 | 0.006 | 0.035 | 0.038 |
| a23 | 0.234 | 1.017 | 0.610 | 1.793 | 0.289 | 1.880 | 0.149 |
| a24 | 0.038 | 0.177 | 0.106 | 0.314 | 0.047 | 0.325 | 0.024 |
| a27 | 0.202 | 0.915 | 0.549 | 1.630 | 0.249 | 1.690 | 0.127 |
| a32 | 0.167 | 0.751 | 0.305 | 1.356 | 0.207 | 1.389 | 0.106 |
| a34 | 0.017 | 0.080 | 0.032 | 0.144 | 0.021 | 0.146 | 0.011 |
| a41 | 0.021 | 0.076 | 0.040 | 1.232 | 0.022 | 0.155 | 0.016 |
| a42 | 0.023 | 0.081 | 0.043 | 1.310 | 0.024 | 0.164 | 0.017 |
| a43 | 0.023 | 0.084 | 0.044 | 1.358 | 0.025 | 0.170 | 0.018 |
| a46 | 0.026 | 0.093 | 0.049 | 1.511 | 0.028 | 0.190 | 0.020 |
| a47 | 0.093 | 0.319 | 0.176 | 5.264 | 0.096 | 0.660 | 0.073 |
| a51 | 0.021 | 0.026 | 0.013 | 0.078 | 0.048 | 0.020 | 0.023 |
| a56 | 0.351 | 0.444 | 0.225 | 1.314 | 0.800 | 0.335 | 0.389 |
| a61 | 0.012 | 0.157 | 0.079 | 0.472 | 0.017 | 0.117 | 0.137 |
| a64 | 0.019 | 0.244 | 0.123 | 0.732 | 0.026 | 0.181 | 0.212 |
| a65 | 0.042 | 0.538 | 0.271 | 1.617 | 0.058 | 0.400 | 0.469 |
| a67 | 0.093 | 1.224 | 0.615 | 3.679 | 0.132 | 0.916 | 1.068 |
| a72 | 0.226 | 0.025 | 0.138 | 1.877 | 0.279 | 1.895 | 0.142 |
| a74 | 0.005 | 0.000 | 0.003 | 0.042 | 0.006 | 0.042 | 0.003 |
| a76 | 0.149 | 0.013 | 0.092 | 1.280 | 0.185 | 1.282 | 0.094 |
| d1 | 1.039 | 0.155 | 0.083 | 0.397 | 0.022 | 0.129 | 0.140 |
| d2 | 0.060 | 0.278 | 0.166 | 0.493 | 0.074 | 0.511 | 0.038 |
| d3 | 0.222 | 1.020 | 0.411 | 1.845 | 0.274 | 1.877 | 0.140 |
| d4 | 0.020 | 0.071 | 0.037 | 1.147 | 0.021 | 0.144 | 0.015 |
| d5 | 0.480 | 0.606 | 0.307 | 1.793 | 1.092 | 0.458 | 0.531 |
| d6 | 0.001 | 0.011 | 0.006 | 0.033 | 0.001 | 0.008 | 0.010 |
| d7 | 0.489 | 0.176 | 0.315 | 3.222 | 0.596 | 3.279 | 0.335 |
| k1 | 0.177 | 0.026 | 0.014 | 0.068 | 0.004 | 0.022 | 0.024 |
| k2 | 0.043 | 0.199 | 0.119 | 0.354 | 0.053 | 0.366 | 0.027 |
| k3 | 0.041 | 0.188 | 0.076 | 0.340 | 0.050 | 0.346 | 0.026 |
| k4 | 0.017 | 0.063 | 0.033 | 1.012 | 0.018 | 0.127 | 0.013 |
| k5 | 0.105 | 0.132 | 0.067 | 0.391 | 0.238 | 0.100 | 0.116 |
| k6 | 0.023 | 0.295 | 0.148 | 0.886 | 0.032 | 0.219 | 0.257 |
| k7 | 0.006 | 0.000 | 0.004 | 0.049 | 0.007 | 0.050 | 0.004 |

Note: Larger values are marked in red.

**Table S13. Local robustness analysis of kinetic parameters in the inflammatory network model with 5% perturbations**

| Parameters | Robustness measure $LR_i$ with respect to different outputs | | | | | | |
|---|---|---|---|---|---|---|---|
| | TNFα | IL-1β | TLR2 | NFκB | CXCL10 | IFN-γ | IL10 |
| a12 | 0.030 | 0.021 | 0.007 | 0.003 | 0.000 | 0.007 | 0.005 |
| a13 | 0.100 | 0.070 | 0.024 | 0.010 | 0.001 | 0.023 | 0.017 |
| a15 | 0.775 | 0.540 | 0.189 | 0.074 | 0.010 | 0.178 | 0.131 |
| a16 | 0.115 | 0.080 | 0.028 | 0.011 | 0.001 | 0.026 | 0.020 |
| a17 | 0.111 | 0.078 | 0.027 | 0.011 | 0.001 | 0.026 | 0.019 |
| a21 | 0.793 | 3.757 | 20.731 | 1.505 | 0.033 | 0.701 | 0.846 |
| a23 | 0.146 | 0.681 | 3.730 | 0.278 | 0.006 | 0.127 | 0.155 |
| a24 | 0.152 | 0.703 | 3.843 | 0.288 | 0.006 | 0.131 | 0.160 |
| a26 | 0.075 | 0.349 | 1.911 | 0.143 | 0.003 | 0.065 | 0.079 |
| a31 | 0.735 | 2.985 | 20.238 | 1.394 | 0.028 | 0.561 | 0.729 |
| a32 | 1.159 | 4.983 | 34.158 | 2.197 | 0.045 | 0.934 | 1.179 |
| a34 | 0.405 | 1.603 | 10.811 | 0.768 | 0.015 | 0.302 | 0.397 |
| a37 | 0.014 | 0.056 | 0.376 | 0.027 | 0.001 | 0.011 | 0.014 |
| a42 | 0.075 | 0.294 | 1.978 | 0.043 | 0.002 | 0.054 | 0.073 |
| a43 | 0.068 | 0.265 | 1.786 | 0.039 | 0.002 | 0.049 | 0.066 |
| a45 | 0.023 | 0.088 | 0.592 | 0.013 | 0.001 | 0.016 | 0.022 |
| a46 | 0.061 | 0.240 | 1.614 | 0.035 | 0.002 | 0.044 | 0.059 |
| a47 | 0.101 | 0.394 | 2.657 | 0.058 | 0.003 | 0.073 | 0.097 |
| a51 | 0.163 | 0.026 | 0.618 | 0.017 | 0.245 | 0.125 | 0.079 |
| a54 | 0.173 | 0.028 | 0.653 | 0.018 | 0.259 | 0.132 | 0.083 |
| a56 | 0.195 | 0.031 | 0.737 | 0.020 | 0.292 | 0.149 | 0.094 |
| a61 | 0.018 | 0.085 | 0.542 | 0.005 | 0.003 | 0.089 | 0.055 |
| a62 | 0.030 | 0.144 | 0.912 | 0.008 | 0.005 | 0.150 | 0.092 |
| a64 | 0.033 | 0.158 | 1.003 | 0.008 | 0.005 | 0.165 | 0.101 |
| a65 | 0.072 | 0.342 | 2.172 | 0.018 | 0.012 | 0.358 | 0.219 |
| a67 | 0.027 | 0.127 | 0.804 | 0.007 | 0.004 | 0.133 | 0.081 |
| a71 | 0.006 | 0.017 | 0.110 | 0.007 | 0.001 | 0.015 | 0.062 |
| a73 | 0.004 | 0.011 | 0.073 | 0.004 | 0.000 | 0.010 | 0.041 |
| a74 | 0.006 | 0.018 | 0.119 | 0.007 | 0.001 | 0.016 | 0.067 |
| a76 | 0.056 | 0.160 | 1.056 | 0.065 | 0.005 | 0.142 | 0.595 |
| d1 | 1.040 | 0.725 | 0.254 | 0.100 | 0.013 | 0.239 | 0.176 |
| d2 | 1.151 | 6.048 | 34.587 | 2.184 | 0.051 | 1.124 | 1.293 |
| d3 | 0.157 | 0.616 | 4.145 | 0.297 | 0.006 | 0.116 | 0.153 |
| d4 | 0.403 | 1.578 | 10.634 | 0.233 | 0.011 | 0.292 | 0.390 |
| d5 | 0.681 | 0.111 | 2.571 | 0.069 | 1.022 | 0.520 | 0.329 |
| d6 | 0.156 | 0.735 | 4.656 | 0.040 | 0.025 | 0.769 | 0.470 |
| d7 | 0.078 | 0.224 | 1.476 | 0.090 | 0.007 | 0.199 | 0.833 |
| k1 | 0.130 | 0.091 | 0.032 | 0.013 | 0.002 | 0.030 | 0.022 |
| k2 | 0.152 | 0.705 | 3.855 | 0.289 | 0.006 | 0.132 | 0.160 |
| k3 | 0.117 | 0.456 | 3.061 | 0.223 | 0.004 | 0.086 | 0.114 |
| k4 | 0.076 | 0.296 | 1.996 | 0.044 | 0.002 | 0.055 | 0.073 |
| k5 | 0.149 | 0.024 | 0.565 | 0.015 | 0.224 | 0.114 | 0.072 |

| | | | | | | | |
|---|---|---|---|---|---|---|---|
| k6 | 0.028 | 0.132 | 0.840 | 0.007 | 0.005 | 0.139 | 0.085 |
| k7 | 0.006 | 0.018 | 0.119 | 0.007 | 0.001 | 0.016 | 0.067 |

Note: Larger values are marked in red.

**Table S14. Local robustness analysis of kinetic parameters in inflammatory network model with 10% perturbations**

| Parameters | Robustness measure $LR_i$ with respect to different outputs | | | | | | |
|---|---|---|---|---|---|---|---|
| | TNFα | IL-1β | TLR2 | NFκB | CXCL10 | IFN-γ | IL10 |
| a12 | 0.030 | 0.021 | 0.007 | 0.003 | 0.000 | 0.007 | 0.005 |
| a13 | 0.102 | 0.071 | 0.025 | 0.010 | 0.001 | 0.023 | 0.017 |
| a15 | 0.792 | 0.552 | 0.193 | 0.076 | 0.010 | 0.182 | 0.134 |
| a16 | 0.118 | 0.082 | 0.029 | 0.011 | 0.002 | 0.027 | 0.020 |
| a17 | 0.114 | 0.079 | 0.028 | 0.011 | 0.001 | 0.026 | 0.019 |
| a21 | 0.791 | 3.952 | 22.217 | 1.502 | 0.034 | 0.736 | 0.866 |
| a23 | 0.150 | 0.707 | 3.895 | 0.284 | 0.006 | 0.132 | 0.159 |
| a24 | 0.155 | 0.718 | 3.932 | 0.294 | 0.006 | 0.134 | 0.163 |
| a26 | 0.077 | 0.357 | 1.956 | 0.146 | 0.003 | 0.067 | 0.081 |
| a31 | 0.730 | 3.187 | 21.909 | 1.385 | 0.029 | 0.597 | 0.749 |
| a32 | 1.157 | 6.255 | 44.509 | 2.194 | 0.050 | 1.160 | 1.320 |
| a34 | 0.408 | 1.676 | 11.387 | 0.774 | 0.015 | 0.315 | 0.407 |
| a37 | 0.015 | 0.057 | 0.384 | 0.028 | 0.001 | 0.011 | 0.014 |
| a42 | 0.077 | 0.300 | 2.025 | 0.044 | 0.002 | 0.056 | 0.074 |
| a43 | 0.069 | 0.271 | 1.830 | 0.040 | 0.002 | 0.050 | 0.067 |
| a45 | 0.023 | 0.090 | 0.605 | 0.013 | 0.001 | 0.017 | 0.022 |
| a46 | 0.063 | 0.245 | 1.652 | 0.036 | 0.002 | 0.045 | 0.061 |
| a47 | 0.103 | 0.404 | 2.723 | 0.060 | 0.003 | 0.075 | 0.100 |
| a51 | 0.167 | 0.027 | 0.632 | 0.017 | 0.251 | 0.127 | 0.081 |
| a54 | 0.176 | 0.028 | 0.667 | 0.018 | 0.265 | 0.135 | 0.085 |
| a56 | 0.199 | 0.032 | 0.753 | 0.020 | 0.299 | 0.152 | 0.096 |
| a61 | 0.018 | 0.087 | 0.554 | 0.005 | 0.003 | 0.091 | 0.056 |
| a62 | 0.031 | 0.147 | 0.932 | 0.008 | 0.005 | 0.154 | 0.094 |
| a64 | 0.034 | 0.162 | 1.025 | 0.009 | 0.006 | 0.169 | 0.103 |
| a65 | 0.074 | 0.350 | 2.223 | 0.019 | 0.012 | 0.365 | 0.223 |
| a67 | 0.027 | 0.130 | 0.821 | 0.007 | 0.004 | 0.136 | 0.083 |
| a71 | 0.006 | 0.017 | 0.113 | 0.007 | 0.001 | 0.015 | 0.064 |
| a73 | 0.004 | 0.011 | 0.074 | 0.005 | 0.000 | 0.010 | 0.042 |
| a74 | 0.006 | 0.018 | 0.121 | 0.007 | 0.001 | 0.016 | 0.068 |
| a76 | 0.057 | 0.163 | 1.079 | 0.066 | 0.005 | 0.146 | 0.608 |
| d1 | 1.064 | 0.741 | 0.260 | 0.102 | 0.014 | 0.244 | 0.180 |
| d2 | 1.174 | 8.360 | 51.844 | 2.230 | 0.060 | 1.537 | 1.563 |
| d3 | 0.161 | 0.680 | 4.659 | 0.304 | 0.008 | 0.126 | 0.161 |
| d4 | 0.409 | 1.627 | 11.003 | 0.242 | 0.011 | 0.301 | 0.398 |
| d5 | 0.696 | 0.114 | 2.624 | 0.070 | 1.045 | 0.532 | 0.336 |
| d6 | 0.159 | 0.751 | 4.759 | 0.041 | 0.026 | 0.787 | 0.480 |
| d7 | 0.080 | 0.228 | 1.507 | 0.092 | 0.007 | 0.204 | 0.852 |
| k1 | 0.133 | 0.093 | 0.032 | 0.013 | 0.002 | 0.031 | 0.023 |

| | | | | | | | |
|---|---|---|---|---|---|---|---|
| k2 | 0.155 | 0.721 | 3.943 | 0.295 | 0.006 | 0.135 | 0.164 |
| k3 | 0.120 | 0.466 | 3.129 | 0.227 | 0.004 | 0.088 | 0.116 |
| k4 | 0.077 | 0.303 | 2.042 | 0.045 | 0.002 | 0.056 | 0.075 |
| k5 | 0.153 | 0.025 | 0.578 | 0.016 | 0.229 | 0.117 | 0.074 |
| k6 | 0.029 | 0.135 | 0.859 | 0.007 | 0.005 | 0.142 | 0.086 |
| k7 | 0.006 | 0.018 | 0.122 | 0.007 | 0.001 | 0.016 | 0.069 |

Note: Larger values are marked in red.

**Table S15. Local robustness analysis of kinetic parameters in inflammatory network model with 20% perturbations**

| Parameters | Robustness measure $LR_i$ with respect to different outputs | | | | | | |
|---|---|---|---|---|---|---|---|
| | TNFα | IL-1β | TLR2 | NFκB | CXCL10 | IFN-γ | IL10 |
| a12 | 0.035 | 0.025 | 0.009 | 0.003 | 0.000 | 0.008 | 0.006 |
| a13 | 0.119 | 0.083 | 0.029 | 0.011 | 0.002 | 0.027 | 0.020 |
| a15 | 0.925 | 0.644 | 0.225 | 0.089 | 0.012 | 0.212 | 0.157 |
| a16 | 0.138 | 0.096 | 0.034 | 0.013 | 0.002 | 0.032 | 0.023 |
| a17 | 0.133 | 0.093 | 0.032 | 0.013 | 0.002 | 0.030 | 0.023 |
| a21 | 0.863 | 4.964 | 29.143 | 1.651 | 0.041 | 0.920 | 1.018 |
| a23 | 0.178 | 1.164 | 7.146 | 0.334 | 0.018 | 0.214 | 0.220 |
| a24 | 0.180 | 0.844 | 4.634 | 0.342 | 0.007 | 0.158 | 0.191 |
| a26 | 0.090 | 0.419 | 2.298 | 0.170 | 0.004 | 0.078 | 0.095 |
| a31 | 0.802 | 4.038 | 28.429 | 1.525 | 0.035 | 0.752 | 0.882 |
| a32 | 2.133 | 41.713 | 327.518 | 4.174 | 0.080 | 7.440 | 5.778 |
| a34 | 0.461 | 2.063 | 14.246 | 0.873 | 0.018 | 0.386 | 0.478 |
| a37 | 0.017 | 0.067 | 0.448 | 0.033 | 0.001 | 0.013 | 0.017 |
| a42 | 0.089 | 0.352 | 2.378 | 0.052 | 0.002 | 0.065 | 0.087 |
| a43 | 0.081 | 0.319 | 2.157 | 0.047 | 0.002 | 0.059 | 0.078 |
| a45 | 0.027 | 0.105 | 0.708 | 0.015 | 0.001 | 0.019 | 0.026 |
| a46 | 0.073 | 0.287 | 1.938 | 0.042 | 0.002 | 0.053 | 0.071 |
| a47 | 0.120 | 0.475 | 3.212 | 0.071 | 0.003 | 0.088 | 0.117 |
| a51 | 0.195 | 0.031 | 0.739 | 0.020 | 0.293 | 0.149 | 0.094 |
| a54 | 0.206 | 0.033 | 0.780 | 0.021 | 0.309 | 0.157 | 0.099 |
| a56 | 0.232 | 0.037 | 0.881 | 0.024 | 0.349 | 0.177 | 0.112 |
| a61 | 0.022 | 0.102 | 0.647 | 0.005 | 0.003 | 0.107 | 0.065 |
| a62 | 0.036 | 0.172 | 1.092 | 0.009 | 0.006 | 0.179 | 0.110 |
| a64 | 0.040 | 0.189 | 1.200 | 0.010 | 0.006 | 0.197 | 0.121 |
| a65 | 0.086 | 0.411 | 2.614 | 0.021 | 0.014 | 0.427 | 0.261 |
| a67 | 0.032 | 0.151 | 0.959 | 0.008 | 0.005 | 0.158 | 0.097 |
| a71 | 0.007 | 0.020 | 0.132 | 0.008 | 0.001 | 0.018 | 0.074 |
| a73 | 0.005 | 0.013 | 0.087 | 0.005 | 0.000 | 0.012 | 0.049 |
| a74 | 0.007 | 0.021 | 0.142 | 0.009 | 0.001 | 0.019 | 0.080 |
| a76 | 0.066 | 0.191 | 1.265 | 0.077 | 0.006 | 0.170 | 0.710 |
| d1 | 1.248 | 0.870 | 0.305 | 0.120 | 0.016 | 0.286 | 0.212 |
| d2 | 1.701 | 26.970 | 187.356 | 3.291 | 0.083 | 4.841 | 3.913 |
| d3 | 0.206 | 1.511 | 11.216 | 0.380 | 0.038 | 0.283 | 0.269 |
| d4 | 0.468 | 1.947 | 13.281 | 0.295 | 0.013 | 0.360 | 0.466 |

| | | | | | | | |
|---|---|---|---|---|---|---|---|
| d5 | 0.816 | 0.135 | 3.061 | 0.082 | 1.226 | 0.624 | 0.394 |
| d6 | 0.187 | 0.881 | 5.586 | 0.050 | 0.030 | 0.922 | 0.563 |
| d7 | 0.093 | 0.267 | 1.759 | 0.108 | 0.008 | 0.239 | 0.998 |
| k1 | 0.155 | 0.108 | 0.038 | 0.015 | 0.002 | 0.036 | 0.026 |
| k2 | 0.181 | 0.846 | 4.648 | 0.343 | 0.008 | 0.158 | 0.192 |
| k3 | 0.140 | 0.546 | 3.675 | 0.265 | 0.005 | 0.103 | 0.136 |
| k4 | 0.090 | 0.355 | 2.399 | 0.053 | 0.002 | 0.066 | 0.087 |
| k5 | 0.178 | 0.029 | 0.675 | 0.018 | 0.268 | 0.136 | 0.086 |
| k6 | 0.033 | 0.158 | 1.005 | 0.008 | 0.005 | 0.165 | 0.101 |
| k7 | 0.008 | 0.022 | 0.142 | 0.009 | 0.001 | 0.019 | 0.080 |

Note: Larger values are marked in red.

**Table S16. Global robustness analysis of initial values in normal network model**

| Outputs | Global robustness measure $GR_i$ with respect to different initial values perturbations | | | Average |
|---|---|---|---|---|
| | 5% | 10% | 20% | |
| TNFα | 3.49E-09 | 1.67E-09 | 9.01E-10 | 2.02E-09 |
| IL-1β | 4.96E-09 | 2.42E-09 | 1.32E-09 | 2.90E-09 |
| TLR2 | 3.14E-09 | 1.52E-09 | 8.28E-10 | 1.83E-09 |
| NFκB | 7.09E-09 | 3.39E-09 | 1.86E-09 | 4.11E-09 |
| CXCL10 | 3.11E-09 | 1.49E-09 | 7.91E-10 | 1.80E-09 |
| IFN-γ | 1.29E-09 | 5.15E-10 | 2.87E-10 | 6.96E-10 |
| IL10 | 3.41E-09 | 1.65E-09 | 8.95E-10 | 1.99E-09 |

**Table S17. Global robustness analysis of initial values in inflammatory network model**

| Outputs | Global robustness measure $GR_i$ with respect to different initial values perturbations | | | Average |
|---|---|---|---|---|
| | 5% | 10% | 20% | |
| TNFα | 1.33E-09 | 3.36E-10 | 1.68E-10 | 6.10E-10 |
| IL-1β | 7.39E-09 | 2.30E-09 | 1.24E-09 | 3.64E-09 |
| TLR2 | 5.27E-08 | 2.02E-08 | 1.09E-08 | 2.79E-08 |
| NFκB | 2.43E-09 | 6.13E-10 | 3.17E-10 | 1.12E-09 |
| CXCL10 | 1.12E-10 | 1.44E-11 | 7.31E-12 | 4.46E-11 |
| IFN-γ | 1.38E-09 | 4.04E-10 | 2.17E-10 | 6.68E-10 |
| IL10 | 1.08E-09 | 9.72E-11 | 5.50E-11 | 4.12E-10 |

**Table S18. Global robustness analysis of kinetic parameters in normal network model**

| Outputs | Global robustness measure $GR_i$ with respect to different parameters perturbations | | | Average |
|---|---|---|---|---|
| | 5% | 10% | 20% | |
| TNFα | 3.60E-09 | 3.34E-09 | 1.68E-09 | 2.87E-09 |
| IL-1β | 5.12E-09 | 4.73E-09 | 2.38E-09 | 4.08E-09 |
| TLR2 | 3.20E-09 | 2.96E-09 | 1.49E-09 | 2.55E-09 |
| NFκB | 7.30E-09 | 6.73E-09 | 3.39E-09 | 5.81E-09 |
| CXCL10 | 3.26E-09 | 3.02E-09 | 1.52E-09 | 2.60E-09 |
| IFN-γ | 1.14E-09 | 1.06E-09 | 5.42E-10 | 9.16E-10 |
| IL10 | 3.52E-09 | 3.25E-09 | 1.64E-09 | 2.80E-09 |

**Table S19. Global robustness analysis of kinetic parameters in inflammatory network model**

| Outputs | Global robustness measure $GR_i$ with respect to different parameters perturbations | | | Average |
|---|---|---|---|---|
| | 5% | 10% | 20% | |
| TNFα | 2.36E-10 | 1.57E-10 | 1.12E-10 | 1.68E-10 |
| IL-1β | 1.55E-09 | 1.05E-09 | 7.57E-10 | 1.12E-09 |
| TLR2 | 1.35E-08 | 9.12E-09 | 6.64E-09 | 9.77E-09 |
| NFκB | 4.07E-10 | 2.66E-10 | 2.01E-10 | 2.92E-10 |
| CXCL10 | 1.12E-11 | 6.48E-12 | 4.37E-12 | 7.36E-12 |
| IFN-γ | 2.67E-10 | 1.83E-10 | 1.33E-10 | 1.94E-10 |
| IL10 | 1.08E-10 | 5.73E-11 | 4.11E-11 | 6.89E-11 |

**Table S20. Spearman correlations between the rate of change of the local network entropies of HDAC4 and those of other proteins**

| | TNFα | IL-1β | TLR2 | NFκB | CXCL10 | IFN-γ | IL10 | COX-2 |
|---|---|---|---|---|---|---|---|---|
| HDAC4 | -1 | -0.5 | -0.5 | -1 | -0.5 | -0.5 | -0.5 | -1 |

**Table S21. Descriptions of the proteins selected from published studies**

| Symbol | Entrez Gene Name | Type |
|---|---|---|
| ABCF1 | ATP-binding cassette, sub-family F (GCN20), member 1 | transporter |
| AFAP1L2 | actin filament associated protein 1-like 2 | other |
| AIMP1 | aminoacyl tRNA synthetase complex-interacting multifunctional protein 1 | cytokine |
| ALOX5 | arachidonate 5-lipoxygenase | enzyme |
| ALOX5AP | arachidonate 5-lipoxygenase-activating protein | other |
| C3AR1 | complement component 3a receptor 1 | G-protein coupled receptor |
| CCL13 | chemokine (C-C motif) ligand 13 | cytokine |
| CCL17 | chemokine (C-C motif) ligand 17 | cytokine |
| CCL19 | chemokine (C-C motif) ligand 19 | cytokine |
| CCL2 | chemokine (C-C motif) ligand 2 | cytokine |
| CCL20 | chemokine (C-C motif) ligand 20 | cytokine |
| CCL24 | chemokine (C-C motif) ligand 24 | cytokine |
| CCL3 | chemokine (C-C motif) ligand 3 | cytokine |
| CCL4 | chemokine (C-C motif) ligand 4 | cytokine |
| CCL5 | chemokine (C-C motif) ligand 5 | cytokine |
| CCL7 | chemokine (C-C motif) ligand 7 | cytokine |
| CCR1 | chemokine (C-C motif) receptor 1 | G-protein coupled receptor |
| CCR3 | chemokine (C-C motif) receptor 3 | G-protein coupled receptor |
| CCR7 | chemokine (C-C motif) receptor 7 | G-protein coupled receptor |
| CD14 | CD14 molecule | transmembrane receptor |
| CD40 | CD40 molecule, TNF receptor superfamily member 5 | transmembrane receptor |
| CEBPB | CCAAT/enhancer binding protein (C/EBP), beta | transcription regulator |
| CIITA | class II, major histocompatibility complex, transactivator | transcription regulator |
| CXCL10 | chemokine (C-X-C motif) ligand 10 | cytokine |
| CXCL11 | chemokine (C-X-C motif) ligand 11 | cytokine |
| CXCL2 | chemokine (C-X-C motif) ligand 2 | cytokine |
| CXCL3 | chemokine (C-X-C motif) ligand 3 | cytokine |

| | | |
|---|---|---|
| CXCL6 | chemokine (C-X-C motif) ligand 6 | cytokine |
| CXCL9 | chemokine (C-X-C motif) ligand 9 | cytokine |
| CXCR4 | chemokine (C-X-C motif) receptor 4 | G-protein coupled receptor |
| DARC | Duffy blood group, chemokine receptor | G-protein coupled receptor |
| ELF3 | E74-like factor 3 (ets domain transcription factor, epithelial-specific ) | transcription regulator |
| FOS | FBJ murine osteosarcoma viral oncogene homolog | transcription regulator |
| HDAC4 | histone deacetylase 4 | transcription regulator |
| HDAC5 | histone deacetylase 5 | transcription regulator |
| HDAC9 | histone deacetylase 9 | transcription regulator |
| IFNA2 | interferon, alpha 2 | cytokine |
| IFNB1 | interferon, beta 1, fibroblast | cytokine |
| IFNG | interferon, gamma | cytokine |
| IL29 | interferon, lambda 1 | cytokine |
| IKBKB | inhibitor of kappa light polypeptide gene enhancer in B-cells, kinase beta | kinase |
| IL10 | interleukin 10 | cytokine |
| IL13 | interleukin 13 | cytokine |
| IL17B | interleukin 17B | cytokine |
| IL1A | interleukin 1, alpha | cytokine |
| IL1B | interleukin 1, beta | cytokine |
| IL1RAP | interleukin 1 receptor accessory protein | transmembrane receptor |
| IL1RN | interleukin 1 receptor antagonist | cytokine |
| IL2 | interleukin 2 | cytokine |
| IL4 | interleukin 4 | cytokine |
| IL5 | interleukin 5 (colony-stimulating factor, eosinophil) | cytokine |
| IL6 | interleukin 6 (interferon, beta 2) | cytokine |
| IL7 | interleukin 7 | cytokine |
| IL8 | interleukin 8 | cytokine |
| IRAK2 | interleukin-1 receptor-associated kinase 2 | kinase |
| IRF3 | interferon regulatory factor 3 | transcription regulator |
| ITCH | itchy E3 ubiquitin protein ligase | enzyme |
| LTA4H | leukotriene A4 hydrolase | enzyme |
| LY96 | lymphocyte antigen 96 | transmembrane receptor |
| MAPK14 | mitogen-activated protein kinase 14 | kinase |
| MECOM | MDS1 and EVI1 complex locus | transcription regulator |
| MEFV | Mediterranean fever | other |
| C3 | complement component 3 | chemical - endogenous mammalian |
| C5 | complement component 5 | chemical - endogenous mammalian |
| NFATC3 | nuclear factor of activated T-cells, cytoplasmic, calcineurin-dependent 3 | transcription regulator |
| NFATC4 | nuclear factor of activated T-cells, cytoplasmic, calcineurin-dependent 4 | transcription regulator |
| NFKB1 | nuclear factor of kappa light polypeptide gene enhancer in B-cells 1 | transcription regulator |
| NFRKB | nuclear factor related to kappaB binding protein | transcription regulator |
| NLRP3 | NLR family, pyrin domain containing 3 | other |
| NOD1 | nucleotide-binding oligomerization domain containing 1 | other |
| PTGS2 | prostaglandin-endoperoxide synthase 2 (prostaglandin G/H synthase and cyclooxygenase) | enzyme |

| | | |
|---|---|---|
| PTX3 | pentraxin 3, long | other |
| PYCARD | PYD and CARD domain containing | transcription regulator |
| RIPK2 | receptor-interacting serine-threonine kinase 2 | kinase |
| SELE | selectin E | transmembrane receptor |
| SERPINA3 | serpin peptidase inhibitor, clade A (alpha-1 antiproteinase, antitrypsin), member 3 | other |
| TLR1 | toll-like receptor 1 | transmembrane receptor |
| TLR2 | toll-like receptor 2 | transmembrane receptor |
| TLR3 | toll-like receptor 3 | transmembrane receptor |
| TLR4 | toll-like receptor 4 | transmembrane receptor |
| TLR5 | toll-like receptor 5 | transmembrane receptor |
| TLR6 | toll-like receptor 6 | transmembrane receptor |
| TLR7 | toll-like receptor 7 | transmembrane receptor |
| TLR9 | toll-like receptor 9 | transmembrane receptor |
| TNFα | tumor necrosis factor | cytokine |
| TNFRSF4 | tumor necrosis factor receptor superfamily, member 4 | transmembrane receptor |
| TNFSF10 | tumor necrosis factor (ligand) superfamily, member 10 | cytokine |
| TNFSF4 | tumor necrosis factor (ligand) superfamily, member 4 | cytokine |
| TOLLIP | toll interacting protein | other |
| TPST1 | tyrosylprotein sulfotransferase 1 | enzyme |

**Table S22. Spearman correlations of the local network entropies between HDAC4, HDAC5, TNFSF10 and three proteins (TNFα, NFκB, COX-2) for HCV infection**

| | HDAC4 | HDAC5 | TNFSF10 |
|---|---|---|---|
| TNFα | -0.5 | -1 | 0.5 |
| NFκB | -0.5 | 0.5 | -1 |
| COX-2 | 1 | 0.5 | 0.5 |

## Supplementary Text:

**Improved conjugate gradient algorithm.** We proposed an improved conjugate gradient method (ICG) to solve the optimization problem in the equation (4) in the main text. The detailed procedure of the algorithm was given below.

Algorithm 1: ICG

Step 1: Obtain the initialization point $x_0$ by using the function *fmincon* in the Matlab toolbox to solve this optimization problem and initialize the iterations to $k$=0;

Step 2: Compute the objective function value $J_\alpha(x_k)$ and the gradient of the objective function as follows:

$$g_k = \nabla J_\alpha(x_k) = \Phi_i x_k - Y_i^{\exp} + \alpha x_k;$$

Step 3: If $\|g_k\|_2 < \varepsilon$, then $x^*=x_k$, and the algorithm is terminated. Otherwise, proceed to Step 4.

Step 4: Adopt the Fletcher-Reeves formula to determine the search direction $d_k$,

$$d_k = \begin{cases} -g_k + \beta_{k-1} d_{k-1}, & k \geq 1 \\ -g_k, & k = 0 \end{cases}$$

where $\beta_{k-1} = \dfrac{g_k^T g_k}{g_{k-1}^T g_{k-1}}$.

Step 5: Use the line search method based on Armilo criteria to select the interation size $\alpha_k = \beta^{m_k}$, where $m_k$ is the smallest non-negative integer that satisfies the following inequality:

$$J_\alpha(x_k + \beta^m d_k) \leq J_\alpha(x_k) + \sigma \beta^m g_k^T d_k,$$

where $\beta \in (0, 1)$, and $\sigma \in (0, 0.5)$.

Step 6: $x_{k+1} = x_k + \alpha_k d_k, k = k+1$, and return to Step 2.

**Nonlinear ODEs models of the two subnetworks.** The ODEs of the two subnetworks are given blow.

(1) The ODEs in inflammatory sub-network

$$\frac{dx_1}{dt} = a_{12}x_2 + \frac{a_{13}x_3^2}{1+x_3^2} + a_{15}x_5 + \frac{a_{16}x_6^2}{1+x_6^2} + \frac{a_{17}x_7^2}{1+x_7^2} - d_1x_1 + k_1$$

$$\frac{dx_2}{dt} = a_{21}x_1 + a_{23}x_3 + \frac{a_{24}x_4^2}{1+x_4^2} + a_{26}x_6 - d_2x_2 + k_2$$

$$\frac{dx_3}{dt} = a_{31}x_1 + a_{32}x_2 + a_{34}x_4 + a_{37}x_7 - d_3x_3 + k_3$$

$$\frac{dx_4}{dt} = \frac{a_{42}x_2^2}{1+x_2^2} + \frac{a_{43}x_3^2}{1+x_3^2} + a_{45}x_5 + a_{46}x_6 + a_{47}x_7 - d_4x_4 + k_4$$

$$\frac{dx_5}{dt} = \frac{a_{51}x_1^2}{1+x_1^2} + \frac{a_{54}x_4^2}{1+x_4^2} + \frac{a_{56}x_6^2}{1+x_6^2} - d_5x_5 + k_5$$

$$\frac{dx_6}{dt} = a_{61}x_1 + a_{62}x_2 + \frac{a_{64}x_4^2}{1+x_4^2} + a_{65}x_5 + a_{67}x_7 - d_6x_6 + k_6$$

$$\frac{dx_7}{dt} = \frac{a_{71}x_1^2}{1+x_1^2} + \frac{a_{73}x_3^2}{1+x_3^2} + \frac{a_{74}x_4^2}{1+x_4^2} + a_{76}x_6 - d_7x_7 + k_7$$

(2) The ODEs in normal sub-network

$$\frac{dx_1}{dt} = \frac{a_{14}x_4^2}{1+x_4^2} + a_{15}x_5 + \frac{a_{16}x_6^2}{1+x_6^2} - d_1x_1 + k_1$$

$$\frac{dx_2}{dt} = a_{23}x_3 + \frac{a_{24}x_4^2}{1+x_4^2} + a_{27}x_7 - d_2x_2 + k_2$$

$$\frac{dx_3}{dt} = a_{32}x_2 + a_{34}x_4 - d_3x_3 + k_3$$

$$\frac{dx_4}{dt} = \frac{a_{41}x_1^2}{1+x_1^2} + \frac{a_{42}x_2^2}{1+x_2^2} + \frac{a_{43}x_3^2}{1+x_3^2} + a_{46}x_6 + a_{47}x_7 - d_4x_4 + k_4$$

$$\frac{dx_5}{dt} = \frac{a_{51}x_1^2}{1+x_1^2} + \frac{a_{56}x_6^2}{1+x_6^2} - d_5x_5 + k_5$$

$$\frac{dx_6}{dt} = a_{61}x_1 + \frac{a_{64}x_4^2}{1+x_4^2} + a_{65}x_5 + a_{67}x_7 - d_6x_6 + k_6$$

$$\frac{dx_7}{dt} = a_{72}x_2 + \frac{a_{74}x_4^2}{1+x_4^2} + a_{76}x_6 - d_7x_7 + k_7$$

In the above ODEs, $x_i$ ($i$=1, 2 , ... , 7) represents the activity of TNFα, IL-1β, TLR2, NFκB, CXCL10, IFN-γ and IL10, respectively.

**DMGBDE algorithm.** The procedure of DMGBDE algorithm is as follows.

## Algorithm 2: DMGBDE algorithm

(1): Initialize the population $\boldsymbol{X}$ and compute the corresponding fitness $\boldsymbol{Xf}$. $MaxFES=n\cdot 10^4$.

(2): Initialize $FES$= 0, $FlagRenew$=1, $nNIMPROVE$=0 and objective function $Fun$.

(3): $VF$ and $VCR$ are initialized to be 0.1+0.8rand($N$, 2) and rand($N$, 2), respectively.

(4): *Option*=*optimset*('*LargeScale*', '*off*', '*HessUpdate*', '*bfgs*', '*TolFun*', 1e-30, '*TolX*', 1e-30);

(5): while $FES \leqq MaxFES$ do

(6): **% Step 1: Perform local search around the searched best individual.**

(7): if *FlagRenew*=1 then

(8): $[Te, Tef] = QNLS(Fun, X_i, Option, n + \left\lfloor \frac{FES}{MaxFES} MaxITER \right\rfloor)$;

(See the Algorithm 3)

(9): $X_* \leftarrow Te, Xf_* \leftarrow Tef$. Renew *FES*.

(10): *FlagRenew*=0.

(11): end if

(12): **% Step 2: Generate trial individuals by using DMM and renew the population.**

(13): for *i*=1,…, *N* do

(14): if $rand \leqq pDEc$ then

(15): $\left[X, Xf, VF, VCR\right] = TrialInd\left(Xf, VF, VCR, 1\right)$.

(16): else

(17): $\left[X, Xf, VF, VCR\right] = TrialInd\left(Xf, VF, VCR, 2\right)$.

(See the Algorithm 4)

(18): end if

(19): $FES \leftarrow FES + 1$. Set *FlagRenew*=1 if the best individual has been renewed.

(20): end for

(21): **% Step 3: Perform local search around other competitive individuals.**

(22): if the best has not been renewed then

(23): *nNIMPROVE*=*nNIMPROVE*+1.

(24): if *nNIMPROVE*>*NNIMPROVE*

(25): for $i = 1, \cdots, \min\{\max\{\lfloor 0.1 \cdot n \rfloor, 3\}, 8\}$ do

(26): Choose the (*i*+1) -th best individual $X_{*(i+1)}$.

(27): $[Te, Tef] = QNLS(Fun, X_{*(i+1)}, Option, n + MaxITER)$;

(See the Algorithm 3)

(28): $X_{*(i+1)} \leftarrow Te, Xf_{*(i+1)} \leftarrow Tef$. Renew *FES*.

(29): end for

(30): *nNIMPROVE*=0, *FlagRenew*=1.

(31): end if

(32): else

(33): *nNIMPROVE*=0.

(34): end if

(35): end while

**Algorithm 3 MATLAB code for quasi-Newton (QN) local search: Sub-algorithm for Algorithm 2**

(1): function $[Te, Tef] = QNLS(Fun, x, Option, NumIter)$

(2): $Option.MaxIter = NumIter;$

(3): $[Te, Tef] = fminunc(Fun, x, Option);$

**Algorithm 4 DMM for generating trial individuals: Sub-algorithm for Algorithm 2**

(1): function $[X, Xf, VF, VCR] = TrialInd(Xf, VF, VCR, co)$

(2): Generate random numbers $rand_1$, $rand_2$ in (0,1).

$$\begin{cases} F = 0.1 + 0.8 rand_1, CR = rand_1 & \text{if } rand_2 \le 0.3, \\ F = VF_{i,co}, CR = VCR_{i,co} & \text{otherwise.} \end{cases}$$

(3): Generate mutation individual:

if $co$=1, $V_i = X_{r_1}^g + F \cdot (X_{r_2}^g - X_{r_3}^g)$,

if $co$=2, $V_{i,j}^{(j)} = X_{r_1,j}^g + F \cdot (X_{r_2,j}^g - X_{r_3,j}^g)$, where $F \in [0,1]$ is the mutation probability.

(4): Perform crossover operation with equation $U_{i,j} = \begin{cases} V_{i,j}, & \text{if } (rand \le CR) \text{ or } (j = rn_i), \\ X_{i,j}^g, & \text{otherwise} \end{cases}$

and generate trial individual *Te*.

(5): if $Fun(Te) < Xf_i$ then

(6): $X_i \leftarrow Te, Xf_i \leftarrow Fun(Te),$

(7): $VF_{i,co} \leftarrow F, VCR_{i,co} \leftarrow CR.$

(8): end if

In the above DMGBDE algorithm, *FES* is the number of function evaluations. $\lfloor A \rfloor$ means rounding number *A* to the nearest integer less than or equal to *A*. The detailed descriptions for the DMGBDE algorithm are available in the literature[1].

## Comparative control study for HCV infection

***Data collection.*** Gene expression profiling of HCV infected Huh7 cells by microarray analysis was retrieved from the Gene Expression Omnibus (GEO) database using the GEO accession number GSE20948[2,3]. A total of 28 RNA samples were analyzed including 3x mock infected samples taken at 6, 12, 18, 24 and 48 hours post-treatment and 3x JFH-1 infected samples taken at 6, 12, 18, 24 and 48 hours post-infection.

***Construction of HCV infection-induced cell-specific normal and inflammatory networks.*** We applied the same procedure of network construction (Supplementary Fig. S1) to construct the normal and inflammatory

networks with HCV infection, respectively. The average relative errors (AREs) of all nodes are less than 0.1 in the constructed normal and inflammatory networks (Supplementary Fig. S21), suggesting that the accuracy and reliability of the constructed networks.

***Both network entropy and other network metrics exhibited no significant differences between the normal and inflammatory networks.*** Based on the same computational and statistical analysis as in the main text, we found that there are not significant differences in the entropies and the variance of protein expression levels between the normal and inflammatory networks for HCV infection (Supplementary Fig. S16), which is very different from those for IAV infection (Figure 3 and Supplementary Fig. S7). In addition, Supplementary Fig. S17 shows that there are not significant differences in these common network metrics between the normal and inflammatory networks. These results indicated that both the network entropy and other network metrics cannot discriminate normal networks from inflammatory networks for HCV infection.

***Identification of protein complexes.*** We also used the TSN-PCD algorithm[4] to identify protein complexes during HCV infection. Surprisingly, the protein complex (TNFSF10/HDAC4/HDAC5), which was predicted to be important for controlling IAV-induced inflammation, has not been identified in the normal and inflammatory networks with HCV infection.

***Correlations.*** Compared to the normal network, the local network entropies of the three proteins (TNFSF10, HDAC4, HDAC5) were increased in the inflammatory networks, while those of TNFα, NFκB and COX-2 were all reduced after HCV infection, which were opposite to those in IAV infection. Moreover, Supplementary Table S22 showed that there were no strong correlations between the entropies of TNFSF10, HDAC4, HDAC5 and those of the three proteins TNFα, NFκB and COX-2.

In summary, these results suggested that the pathogenesis of HCV infection is quite different from that of IAV infection. Our findings in this study are specific to the pathogenesis of IAV disease. However, our investigation supports the quantitative analysis of applying network-based approaches to elucidate the characteristics of infectious diseases and provide a rationale for developing specific intervention strategies to reduce the risk of infectious diseases. These findings can serve as a significant foundation for further exploring the molecular mechanisms of other infectious diseases and developing control strategies.


1. Xie, W., Yu, W. & Zou, X. Diversity-maintained differential evolution embedded with gradient-based local search. *Soft Comput* **17,** 1511-1535(2013).
2. Barrett, T. *et al.* NCBI GEO: archive for functional genomics data sets--update. *Nucleic Acids Res* **41**, D991-995 (2013).
3. Blackham, S. *et al.* Gene expression profiling indicates the roles of host oxidative stress, apoptosis, lipid metabolism, and intracellular transport genes in the replication of hepatitis C virus. *J Virol* **84**, 5404-5414 (2010).
4. Li, M., Wu, X., Wang, J. & Pan, Y. Towards the identification of protein complexes and functional modules by. *BMC Bioinformatics* **13**, 109 (2012).